3. Results

3.1 Preparation of oxalato complexes

$K_3[Cr(C_2O_4)_3]\cdot 3H_2O$ and $K_3[Al(C_2O_4)_3]\cdot 3H_2O$ complexes were prepared according to the literature procedure (Booth H.S., 1939). Both complexes are readily soluble in water. The products were synthesized by mixing small amount of $K_3[Cr(C_2O_4)_3]\cdot 3H_2O$ with $K_3[Al(C_2O_4)_3]\cdot 3H_2O$ and NaCl at room temperature. Three types of crystals were obtained, two with dark red color almost black and the other was blue color. They are designated as RedCubic, RedRhombo, and Blue. The three complexes were studied for their solubility in various solvents. The results data are summarized in Table 2.

Table 2 The solubility of RedCubic, RedRhombo and Blue crystals.

Solvents	Solubility		
	RedCubic	RedRhombo	Blue
Hexane	-	-	-
Toluene	-	-	-
Dichloromethan	+	+	+
Acetone	+	+	+
Dimethylformamide	+	+	+
Acetonitrile	+	+	+
Ethanol	+	+	+
Methanol	++	++	++
Water	+++	+++	+++

- insoluble, + slightly soluble, ++ more soluble, +++ readily soluble

0.0012 g. of complexes were tested their solubility in 10 mL of various solvents. The symbol of solubility, + represents the partial solubility of less than 0.0005 g. and ++ represents better solubility in the range 0.005-0.008 g. The +++ represents 0.0012 g. of those complexes completely soluble in 10 mL of solvents.

The products were also characterized by other techniques such as, scanning electron microanalysis/ energy dispersive x-ray fluorescence(SEM/EDX), inductively coupled plasma-atomic emission spectroscopy(ICP-AES), single crystal x-ray diffraction, uv-visible absorption spectroscopy(UV-Vis), fourier transformed infrared spectrometry(FT-IR), x-ray powder diffraction(XRD), thermogravimetry analyzer (TGA), and differential scanning calorimeter(DSC). The results are shown below.

3.2 Products Characterizations

3.2.1 Titration technique

The contents of oxalate group in oxalate complexes were determined by titration technique with standard $KMnO_4$ and the results are shown in Table 3.

Table 3 The content of oxalate group by titration technique

compound	Calculated(%)	Found(%)***
$K_2C_2O_4.H_2O$	47.76	47.72
$K_3[Al(C_2O_4)_3]\cdot 3H_2O$	57.12	57.32
$K_3[Cr(C_2O_4)_3]\cdot 3H_2O$	54.16	*
RedCubic	**	57.62
RedRhombo	55.51	55.73
Blue	**	55.47

*The percentage of oxalate group in $K_3[Cr(C_2O_4)_3].3H_2O$ could not be determined due to mixed color at the end point. (Interference from the yellow color of Cr^{3+} ion at the end point.)

** The percentage could not be calculated since the structure could not be solved.

*** Average of 8 times.

3.2.2 Elemental analysis

The elemental analyses (K, Na, Cr, Al) in oxalato complexes by inductively coupled plasma atomic emission spectroscopy (ICP-AES) are listed in

Table 4. The content C, H, and O in oxalato complexes were investigated by CHNS-O analyzer. The results are shown in Table 5.

Table 4 The percentage of element (K, Na, Cr, Al) in oxalato complexes by ICP-AES

complex	K	Na	Cr	Al
$K_3[Al(C_2O_4)_3]\cdot 3H_2O$	24.54 (25.37)	-	-	4.78 (5.84)
$K_3[Cr(C_2O_4)_3]\cdot 3H_2O$	24.16 (24.07)	-	10.24 (10.67)	-
RedCubic	1.33	8.99	0.51	4.56
RedRhombo	25.91 (25.99)	0.16 (0.00)	0.34 (0.33)	4.80 (5.51)
Blue	23.90	ND	0.59	4.52

ND = not detectable

Table 5 The percentage of element (C, H, and O) in oxalato complexes by elemental analyzer (CHNS-O)

complex	C	H	O
$K_3[Al(C_2O_4)_3]\cdot 3H_2O$	14.95 (15.59)	1.02 (1.31)	51.04 (51.90)
$K_3[Cr(C_2O_4)_3]\cdot 3H_2O$	14.24 (14.79)	1.13 (1.24)	48.89 (49.24)
RedCubic	16.71	1.58	50.77
RedRhombo	15.65 (15.14)	1.08 (1.26)	49.62 (50.47)
Blue	10.19	1.02	39.78

3.2.3 X-ray single crystal data of $K_{18}\{K[Al_{0.97}Cr_{0.03}(C_2O_4)_3]_6\}Cl.18H_2O$ (RedRhombo)

The single crystals of $K_{18}\{K[Al_{0.97}Cr_{0.03}(C_2O_4)_3]_6\}Cl.18H_2O$ complex were obtained by small amount of $K_3[Cr(C_2O_4)_3]\cdot 3H_2O$ with $K_3[Al(C_2O_4)_3]\cdot 3H_2O$ and NaCl and were grown in water by slow solvent evaporation at room temperature. The unit cell parameters and intensity data were collected at 293 K on a 4k Bruker SMART APEX CCD area-detector diffractometer with graphite monochromated MoK_α radiation (λ = 0.71073 Å) (at a detector distance of 6.0 cm) using SMART program (Bruker, 2000). A fullsphere of the reciprocal space was covered by a combination of three sets of exposures; each set had a different ϕ angle (0, 120, 240°) and each exposure of 10s covered 0.3° in ω. Raw data frame integration was performed with SAINT (Bruker, 2000), with also applied correction for Lorentz and polarization effects. An empirical absorption correction by using the SADABS program (Bruker,2000) was applied, which resulted in transmittion coefficients ranging from 0.905 to 1.000. A total of 16191 reflections (2595 independent reflections, R_{int}= 0.0245) were collected in the range $2.22° < \theta < 24.70°$. This structure was solved by Direct methods using SHLLXTL-PC V6.12 software package (Bruker, 2000) and refined by full matrix least-squares method based on $|F|$ with anisotropic thermal parameters for all non-hydrogen atoms by using XTAL3.7 program system (Hall, et. al., 1999). The hydrogen atoms were found by Fourier maps and refine isotropically. The crystal data and collected parameters are listed in Table 6. Selected bond distances are listed in Table 7. Bond angles are listed in Table 8. View of molecular unit of this complex is shown in Figure 1.

Table 6 Crystal data and structure refinement for $K_{18}\{K[Al_{0.97}Cr_{0.03}(C_2O_4)_3]_6\}Cl.18H_2O$ (RedRhombo)

Crystal parameters	$K_{18}\{K[Al_{0.97}Cr_{0.03}(C_2O_4)_3]_6\}Cl.18H_2O$	
Empirical formula	$C_{36}H_{36}Al_{5.82}Cl_1Cr_{0.18}K_{19}O_{90}$	
	(Population; Al = 0.97, Cr = 0.03)	
Formula weight	2853.30	
Temperature	293(2) K	
Wavelength	0.71073 Å	
Crystal system	Rhombohedral	
Space group	$R\bar{3}$ (No. 148)	
Unit cell dimensions	a = 28.321(2) Å	$\alpha = 90^\circ$.
	b = 28.321(2) Å	$\beta = 90^\circ$
	c = 9.867(1) Å	$\gamma = 120^\circ$
Volume	6853.6(1) $Å^3$	
Z	18	
Density (calculated)	2.074 Mg/m^3	
Absorption coefficient	1.11 mm^{-1}	
F(000)	4079	
Crystal size	0.262 x 0.147 x 0.118 mm^3	
Theta range for data collection	2.22 to 24.70°	
Index ranges	$-33 \leq h \leq 33, -33 \leq k \leq 33, -11 \leq l \leq 11$	
Reflections collected	16191	
Independent reflections	2595 [R(int) = 0.0245]	
Completeness to $\theta = 24.70^\circ$	99.8 %	

Absorption correction	Semi-empirical from equivalents
Max. and min. transmission	1.00 and 0.905
Refinement method	Full-matrix least-squares on F^2
Data / restraints / parameters	2595 / 0 / 237
Goodness-of-fit on F^2	1.016
Final R indices for 2399 reflections [$I>2\sigma(I)$]	$R1$ = 0.0424, $wR2$ = 0.1209
R indices (for 2595 reflection)	$R1$ = 0.0456, $wR2$ = 0.1235
Extinction coefficient	0.00029(1)
Largest diff. peak	0.490 e. Å $^{-3}$

Table 7 The selected bond distances(Å) of $K_{18}\{K[Al_{0.97}Cr_{0.03}(C_2O_4)_3]_6\}Cl.18H_2O$

Atoms	Distances (Å)
K(1)-O(14)	2.400(3)
K(1)-O(14)	2.400(3)
K(1)-O(14)	2.400(3)
K(1)-O(14)	2.400(3)
K(1)-O(14)	2.399(3)
K(1)-O(14)	2.400(3)
Al(1)-O(1)	1.890(3)
Al(1)-O(2)	1.908(3)
Al(1)-O(3)	1.894(3)
Al(1)-O(4)	1.909(3)
Al(1)-O(5)	1.895(3)
Al(1)-O(6)	1.895(3)
Cr(1)-O(1)	1.890(3)
Cr(1)-O(2)	1.908(3)
Cr(1)-O(3)	1.894(3)
Cr(1)-O(4)	1.909(3)
Cr(1)-O(5)	1.895(3)
Cr(1)-O(6)	1.895(3)
C(1)-C(2)	1.554(6)
C(1)-O(1)	1.291(5)
C(1)-O(11)	1.221(5)
C(2)-O(2)	1.275(5)
C(2)-O(12)	1.225(5)

Table 7 (Continued)

C(3)-C(4)	1.551(6)
C(3)-O(3)	1.276(5)
C(3)-O(13)	1.223(5)
C(4)-O(4)	1.280(5)
C(4)-O(14)	1.231(5)
C(5)-C(6)	1.546(6)
C(5)-O(5)	1.283(5)
C(5)-O(15)	1.223(5)
C(6)-O(6)	1.293(5)
C(6)-O(16)	1.212(5)
K(3)-O(7)	2.640(4)

Table 8 Bond Angles (°) of $K_{18}\{K[Al_{0.97}Cr_{0.03}(C_2O_4)_3]_6\}Cl.18H_2O$

Atoms	Angles (°)
O(14)-K(1)-O(14)	95.6(1)
O(14)-K(1)-O(14)	95.7(1)
O(14)-K(1)-O(14)	180.0000
O(14)-K(1)-O(14)	84.4(1)
O(14)-K(1)-O(14)	84.4(1)
O(14)-K(1)-O(14)	95.6(1)
O(14)-K(1)-O(14)	84.3(1)
O(14)-K(1)-O(14)	180.0000
O(14)-K(1)-O(14)	84.3(1)
O(14)-K(1)-O(14)	84.4(1)
O(14)-K(1)-O(14)	84.4(1)
O(14)-K(1)-O(14)	180.0000
O(14)-K(1)-O(14)	95.7(1)
O(14)-K(1)-O(14)	95.6(1)
O(14)-K(1)-O(14)	95.7(1)
O(1)-Al(1)-O(2)	84.4(1)
O(1)-Al(1)-O(3)	89.7(1)
O(1)-Al(1)-O(4)	171.4(1)
O(1)-Al(1)-O(5)	92.6(2)
O(1)-Al(1)-O(6)	94.8(1)
O(2)-Al(1)-O(3)	97.5(1)
O(2)-Al(1)-O(4)	90.1(2)
O(2)-Al(1)-O(5)	171.8(2)

Table 8 (Continued)

O(2)-Al(1)-O(6)	88.6(1)
O(3)-Al(1)-O(4)	84.4(1)
O(3)-Al(1)-O(5)	90.1(1)
O(3)-Al(1)-O(6)	172.8(1)
O(4)-Al(1)-O(5)	93.7(1)
O(4)-Al(1)-O(6)	91.7(1)
O(5)-Al(1)-O(6)	84.0(1)
O(1)-Cr(1)-O(2)	84.4(1)
O(1)-Cr(1)-O(3)	89.7(1)
O(1)-Cr(1)-O(4)	171.4(1)
O(1)-Cr(1)-O(5)	92.6(2)
O(1)-Cr(1)-O(6)	94.8(1)
O(2)-Cr(1)-O(3)	97.5(1)
O(2)-Cr(1)-O(4)	90.1(2)
O(2)-Cr(1)-O(5)	171.8(2)
O(2)-Cr(1)-O(6)	88.6(1)
O(3)-Cr(1)-O(4)	84.4(1)
O(3)-Cr(1)-O(5)	90.1(1)
O(3)-Cr(1)-O(6)	172.8(1)
O(4)-Cr(1)-O(5)	93.7(1)
O(4)-Cr(1)-O(6)	91.7(1)
O(5)-Cr(1)-O(6)	84.0(1)
C(2)-C(1)-O(1)	112.8(4)
C(2)-C(1)-O(11)	121.3(4)
O(1)-C(1)-O(11)	125.8(6)

Table 8 (Continued)

C(1)-C(2)-O(2)	112.9(4)
C(1)-C(2)-O(12)	120.7(4)
O(2)-C(2)-O(12)	126.3(6)
Al(1)-O(1)-Cr(1)	.0(1)
Al(1)-O(1)-C(1)	114.7(4)
Cr(1)-O(1)-C(1)	114.7(4)
Al(1)-O(2)-Cr(1)	.00(7)
Al(1)-O(2)-C(2)	114.7(4)
Cr(1)-O(2)-C(2)	114.7(4)
C(4)-C(3)-O(3)	113.2(4)
C(4)-C(3)-O(13)	120.1(4)
O(3)-C(3)-O(13)	126.7(4)
C(3)-C(4)-O(4)	113.0(4)
C(3)-C(4)-O(14)	119.4(4)
O(4)-C(4)-O(14)	127.6(4)
Al(1)-O(3)-Cr(1)	.0(1)
Al(1)-O(3)-C(3)	114.6(2)
Cr(1)-O(3)-C(3)	114.6(2)
Al(1)-O(4)-Cr(1)	.00(7)
Al(1)-O(4)-C(4)	114.2(3)
Cr(1)-O(4)-C(4)	114.2(3)
K(1)-O(14)-C(4)	123.0(3)
C(6)-C(5)-O(5)	112.6(4)
C(6)-C(5)-O(15)	121.6(4)
O(5)-C(5)-O(15)	125.8(4)

Table 8 (Continued)

C(5)-C(6)-O(6)	112.5(4)
C(5)-C(6)-O(16)	121.7(4)
O(6)-C(6)-O(16)	125.8(4)
Al(1)-O(5)-Cr(1)	.0(1)
Al(1)-O(5)-C(5)	115.4(3)
Cr(1)-O(5)-C(5)	115.4(3)
Al(1)-O(6)-Cr(1)	.0000
Al(1)-O(6)-C(6)	115.2(3)
Cr(1)-O(6)-C(6)	115.2(3)

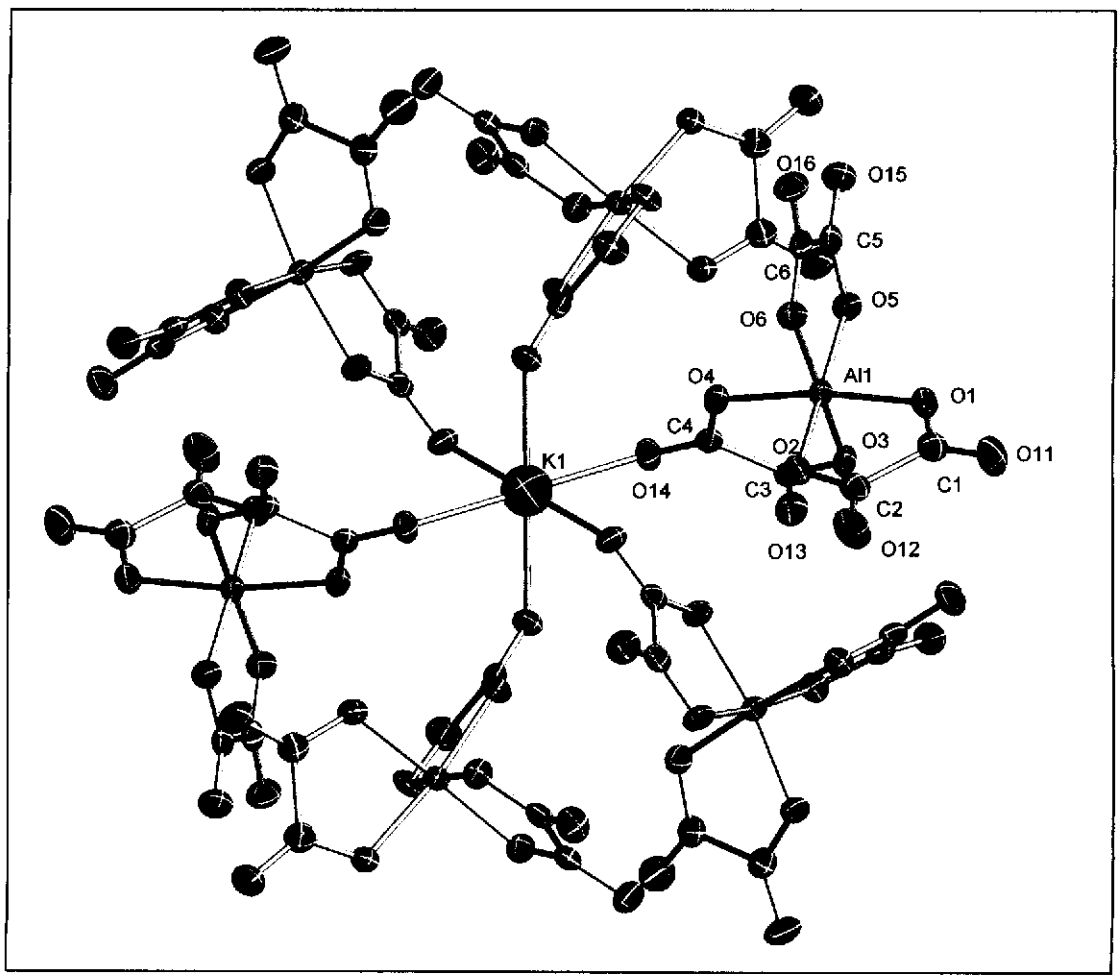

Figure 1 The 50 % thermal ellipsoid of core structure of $K_{18}\{K[Al_{0.97}Cr_{0.03}(C_2O_4)_3]_6\}$ $Cl.18H_2O$ complex molecule plot (all counterions, H_2O, and H atoms are omitted for clarity).

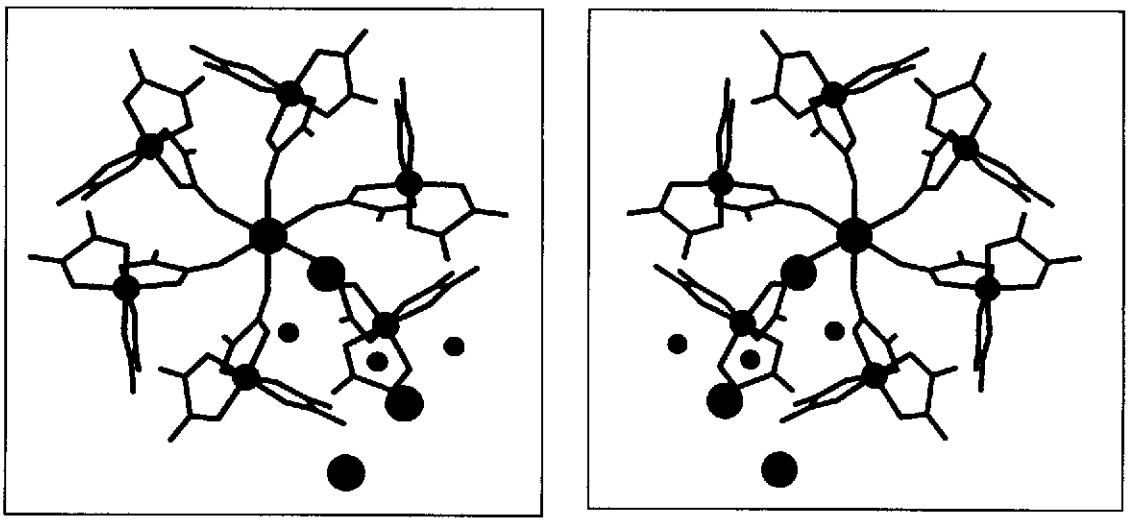

Figure 2 Two 180° views of complex molecule (H atoms are omitted for clarity) ;
Green ball = Cl^-, Green capped sticks (oxalate ring) = C, Blue ball = K,
Violet ball = Al (97.00 %) and Cr (3.00%), Red ball = O (O from H_2O).

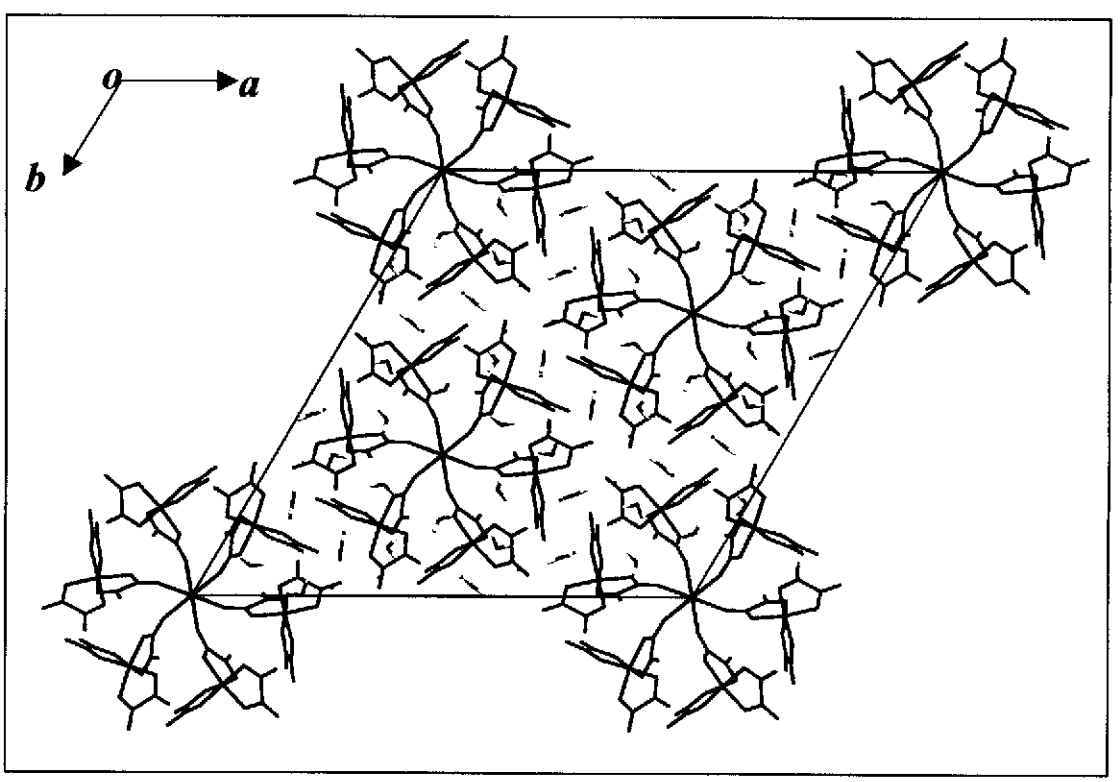

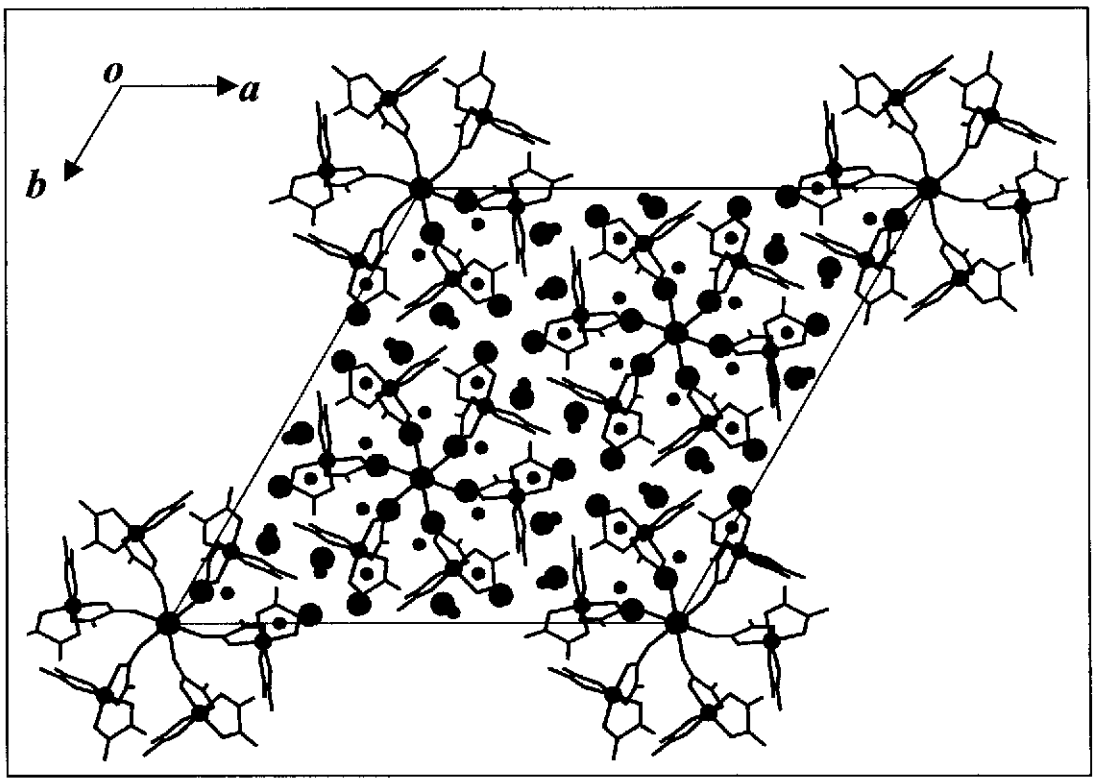

Figure 3 Two views of unit cell plotted down *c* axis:

Top view: Green = Cl^-, Blue = K, Violet = Al (97.00 %) and Cr (3.00%), Red = O, Green (in oxalate ring) = C, Gray = H atom

Bottom View: Green ball = Cl^-, Blue ball and Bule capped sticks = K, Violet ball = Al (97.00 %) and Cr (3.00%), Red capped sticks = O, Green capped sticks = C (H atoms are excluded for clarity).

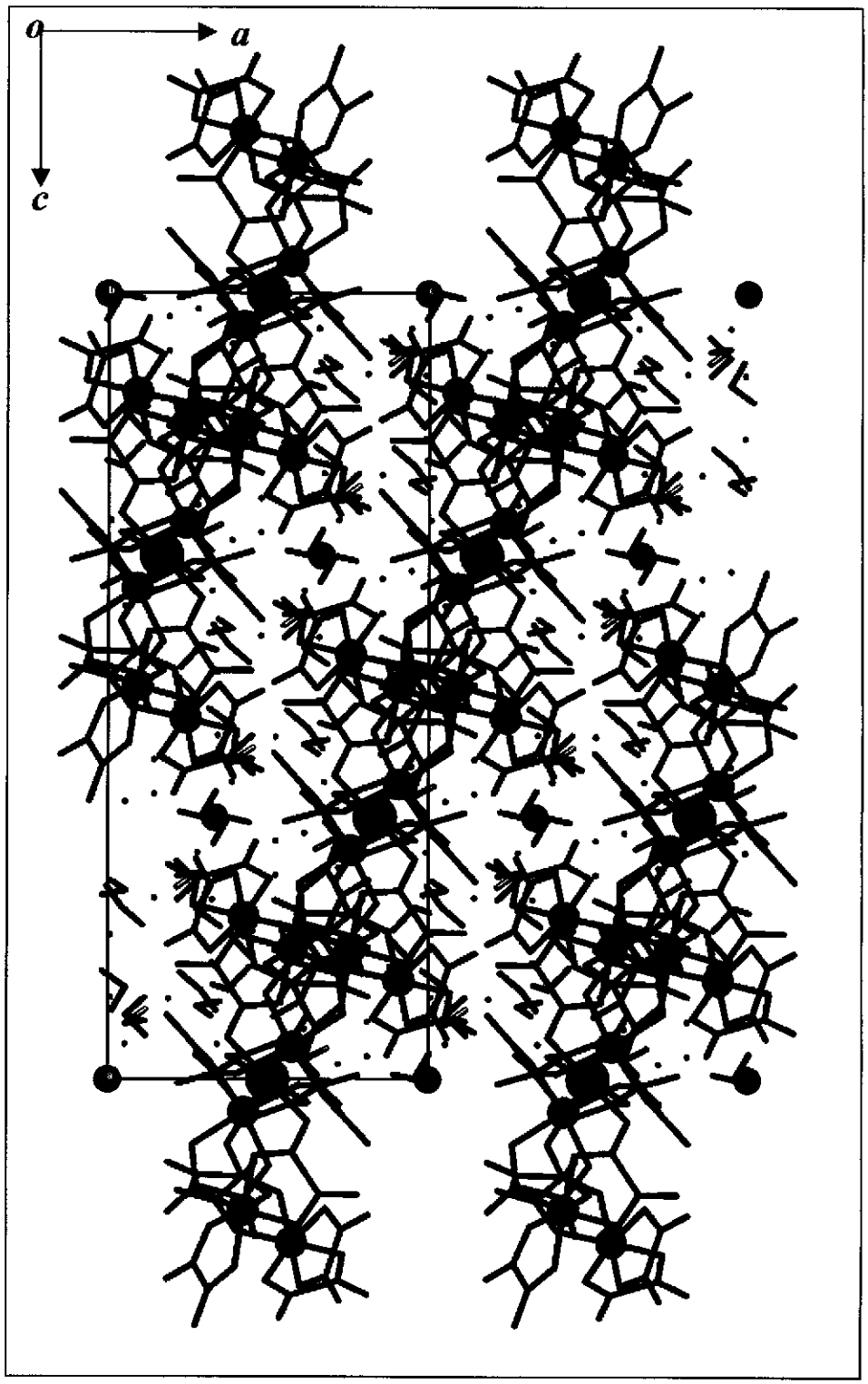

Figure 4 Unit cell plotted down *b* axis: Green ball = Cl^-, Blue ball and Bule capped sticks = K, Violet balls = Al (97.00 %) and Cr (3.00%), Red capped sticks = O, Grey capped sticks = H, Green capped sticks = C.

3.2.4 UV-Visible absorption spectroscopy

Oxalic acid was studied by UV-Visible spectroscopy. The solution absorption spectrum of this compound in water was recorded in the range 200-800 nm and shown in Figure 5.

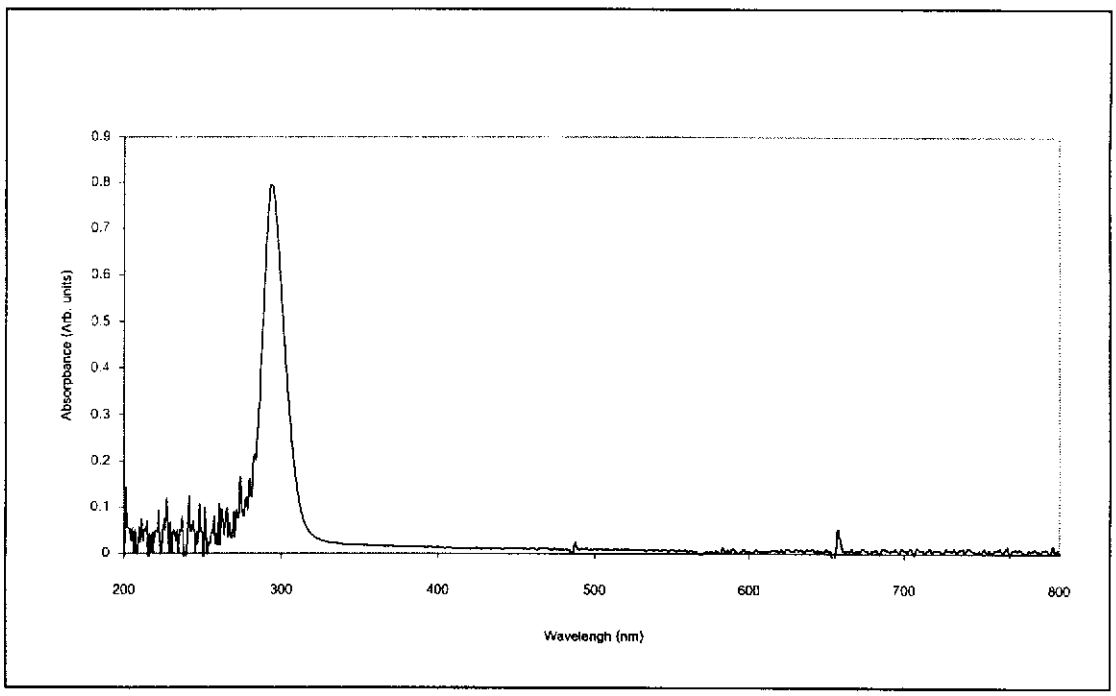

Figure 5 UV-Visible absorption spectrum of oxalic acid in water

RedCubic, RedRhombo, and Blue complexes were studied by UV-Visible spectroscopy. The absorption spectra of the complexes were measured at ambient temperature in the range 200-800 nm for aqueous solution, and 240-800 nm for solid. Their crystal and solution spectra are shown in Figures 6-7, and the maximum bands are summarized in Table 9.

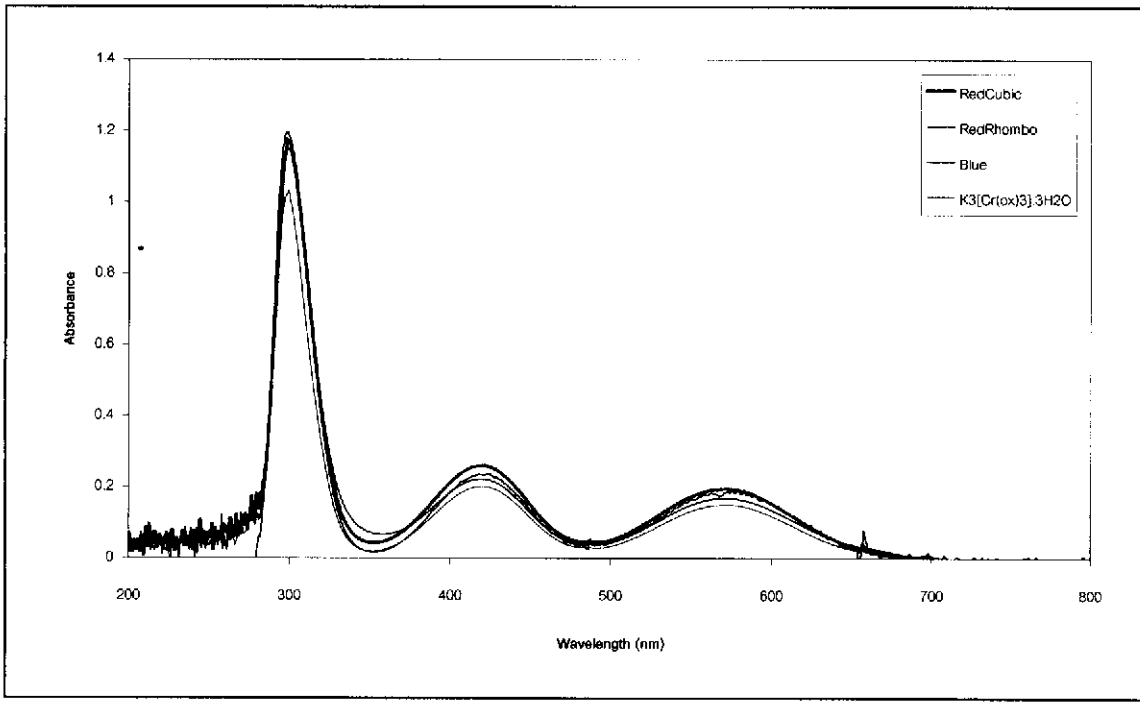

Figure 6 UV-Visible absorption spectra of RedCubic, RedRhombo, Blue, and $K_3[Cr(C_2O_4)_3].3H_2O$ in aqueous solution

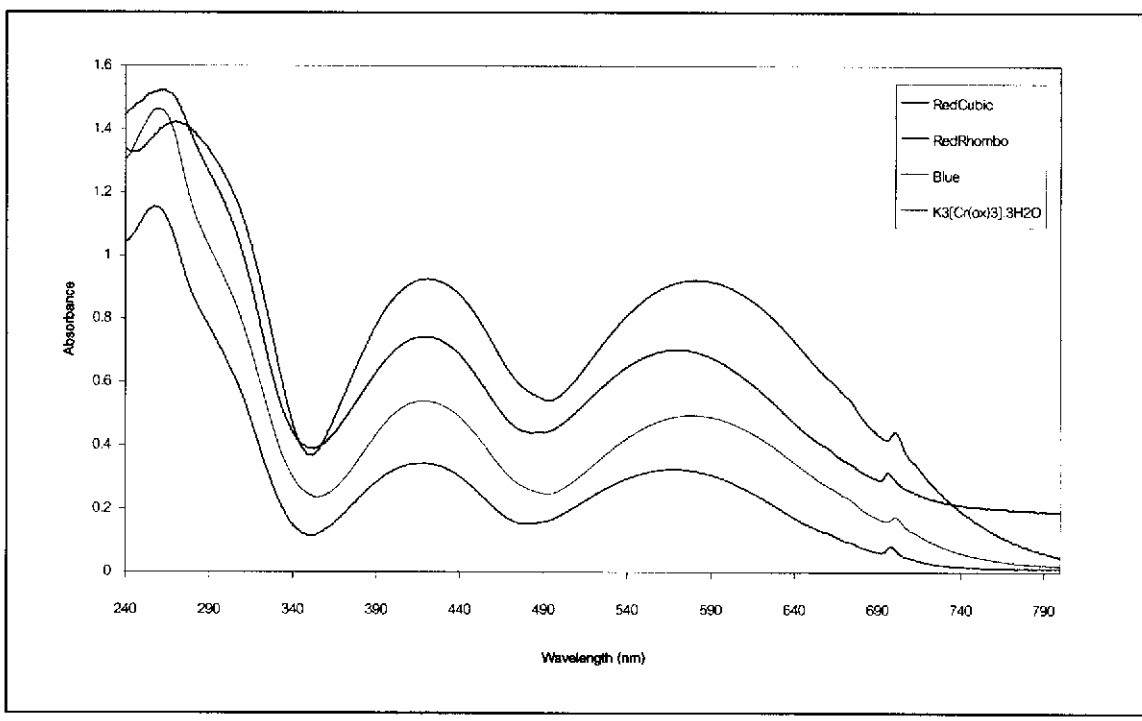

Figure 7 UV-Visible absorption spectra of RedCubic, RedRhombo, Blue, and $K_3[Cr(C_2O_4)_3].3H_2O$ in solid state by diffuse reflectance method

Table 9 Absorption bands of RedCubic, RedRhombo, Blue, and $K_3[Cr(C_2O_4)_3]\cdot 3H_2O$

Complex	Phase	Absorption band (nm)		
		ν_3	ν_2	ν_1
RedCubic	Solution	299	419	572
	Solid	263	421	571
RedRhombo	Solution	299	424	579
	Solid	257	419	567
Blue	Solution	299	419	572
	Solid	269	421	579
$K_3[Cr(C_2O_4)_3]\cdot 3H_2O$	Solution	299	420	572
	Solid	258	420	580

3.2.5 Infrared spectrometry

IR is a useful technique to identify the functional group in compounds. Calibration of the frequency reading was made with polystyrene film and shown in Figure 8.

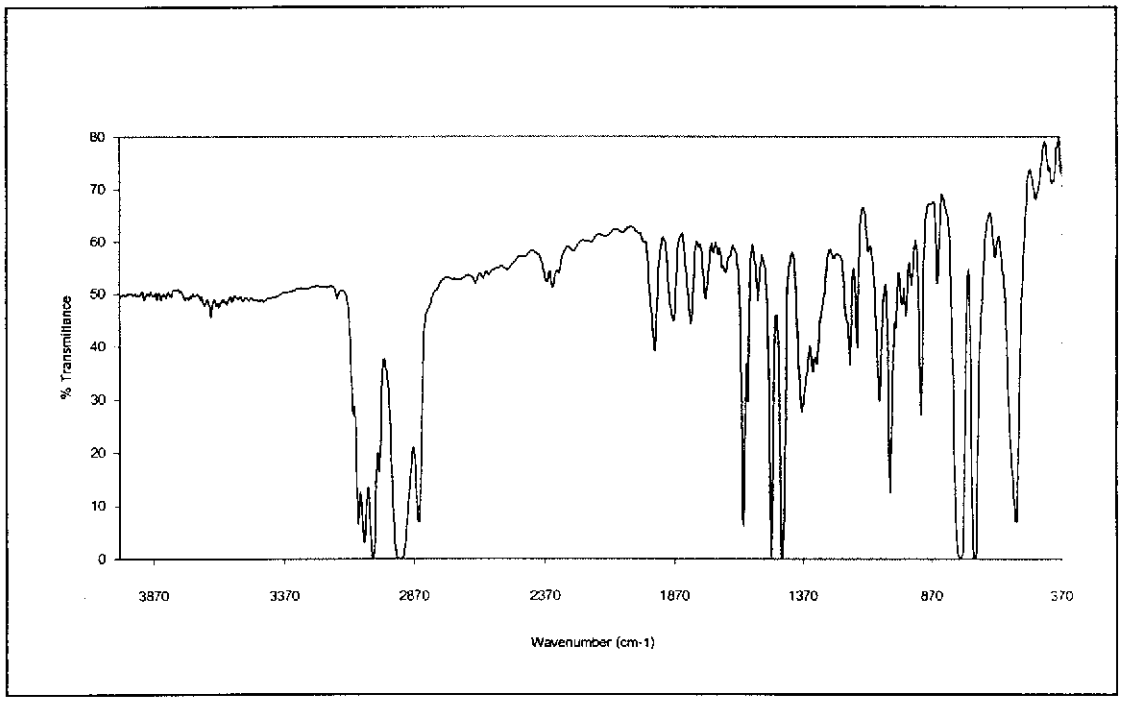

Figure 8 IR spectrum of polystyrene

IR spectra of $K_3[Cr(C_2O_4)_3]\cdot 3H_2O$, $K_3[Al(C_2O_4)_3]\cdot 3H_2O$, RedCubic, RedRhombo, and Blue are shown in Figures 9-14 and summarized in Table 10.

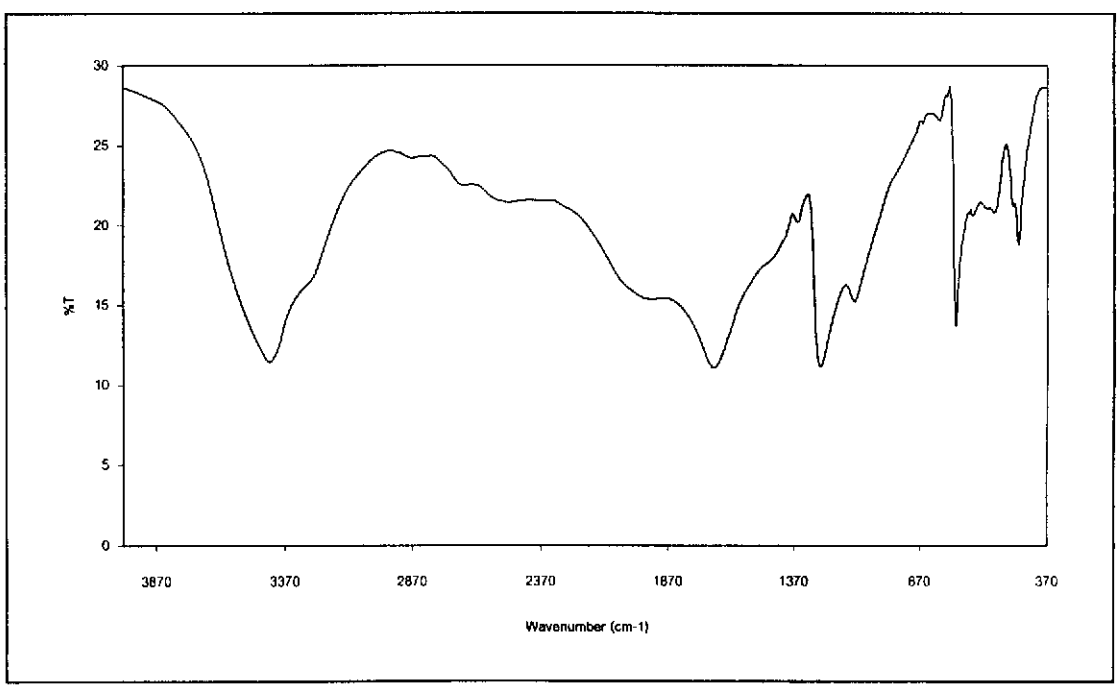

Figure 9 IR spectrum of oxalic acid (KBr disc)

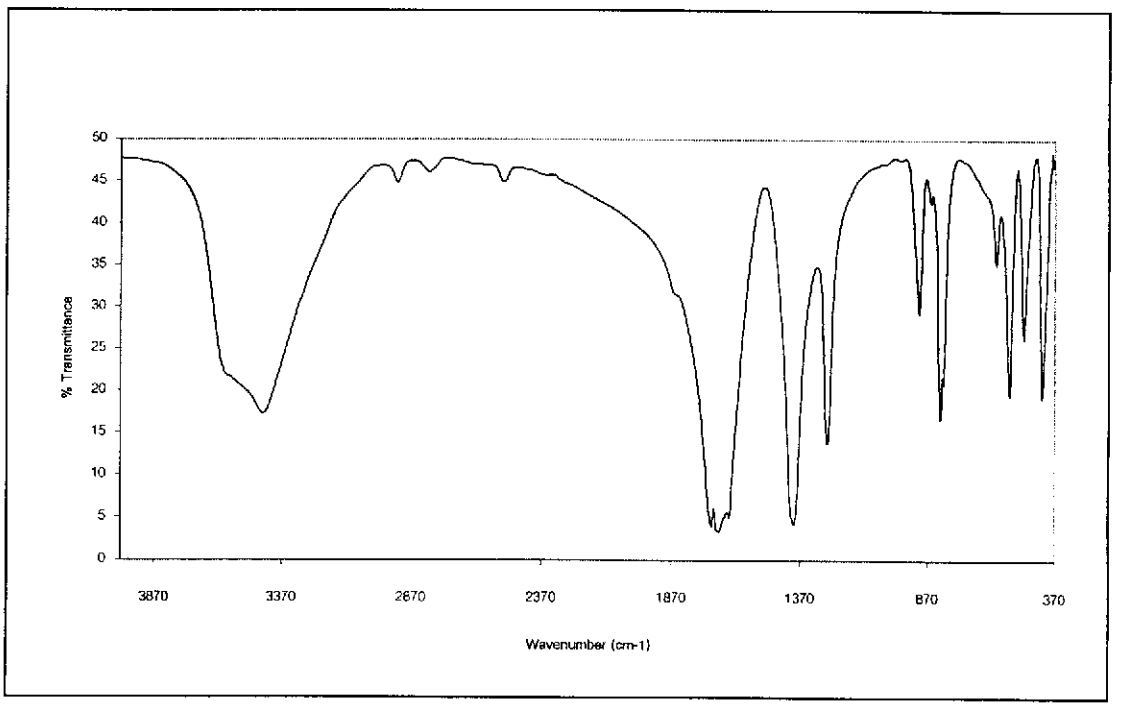

Figure 10 IR spectrum of $K_3[Cr(C_2O_4)_3]\cdot 3H_2O$ (KBr disc)

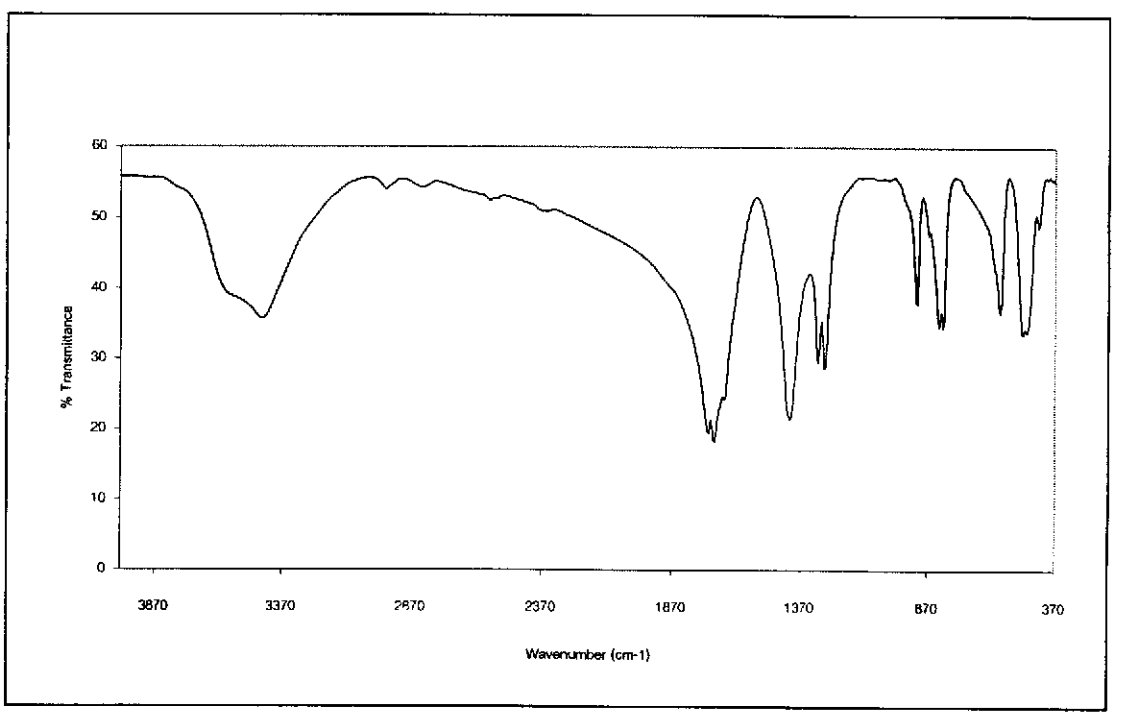

Figure 11 IR spectrum of $K_3[Al(C_2O_4)_3]\cdot 3H_2O$ (KBr disc)

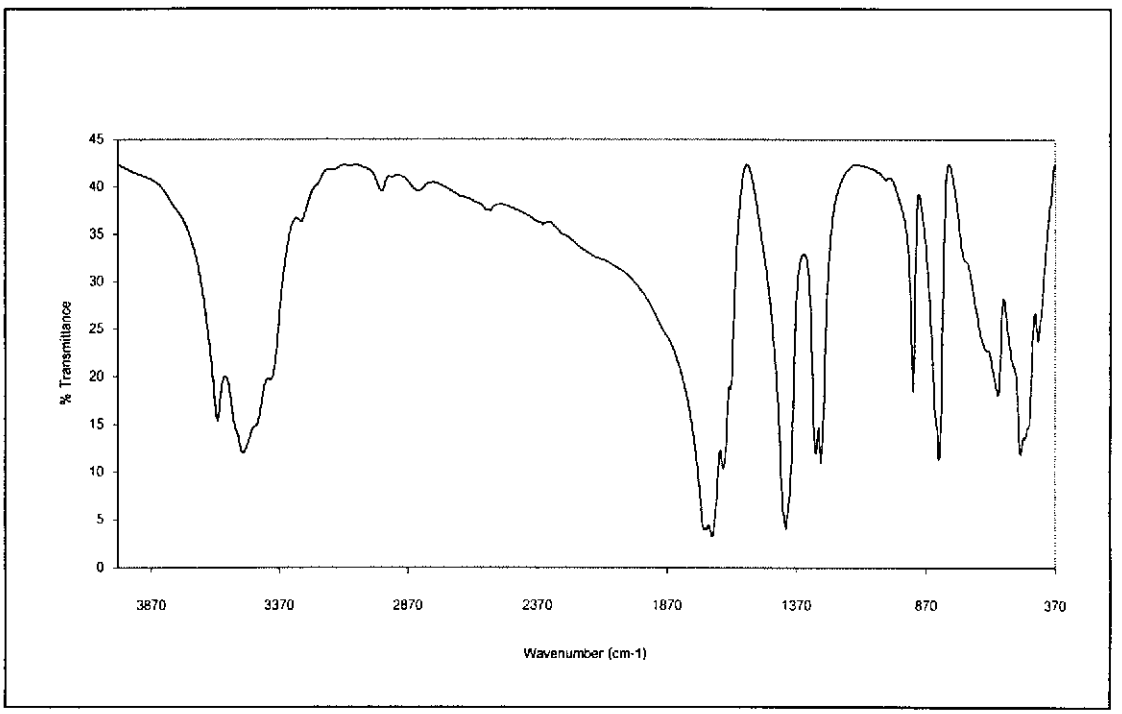

Figure 12 IR spectrum of RedCubic complex (KBr disc)

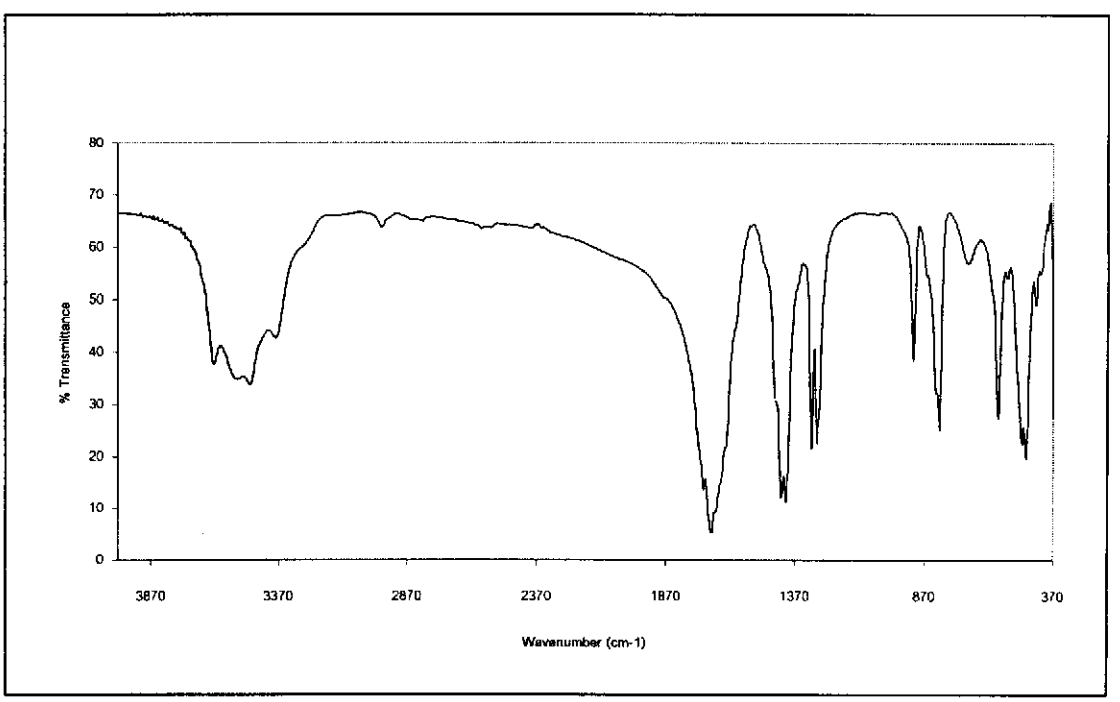

Figure 13 IR spectrum of RedRhombo complex (KBr disc)

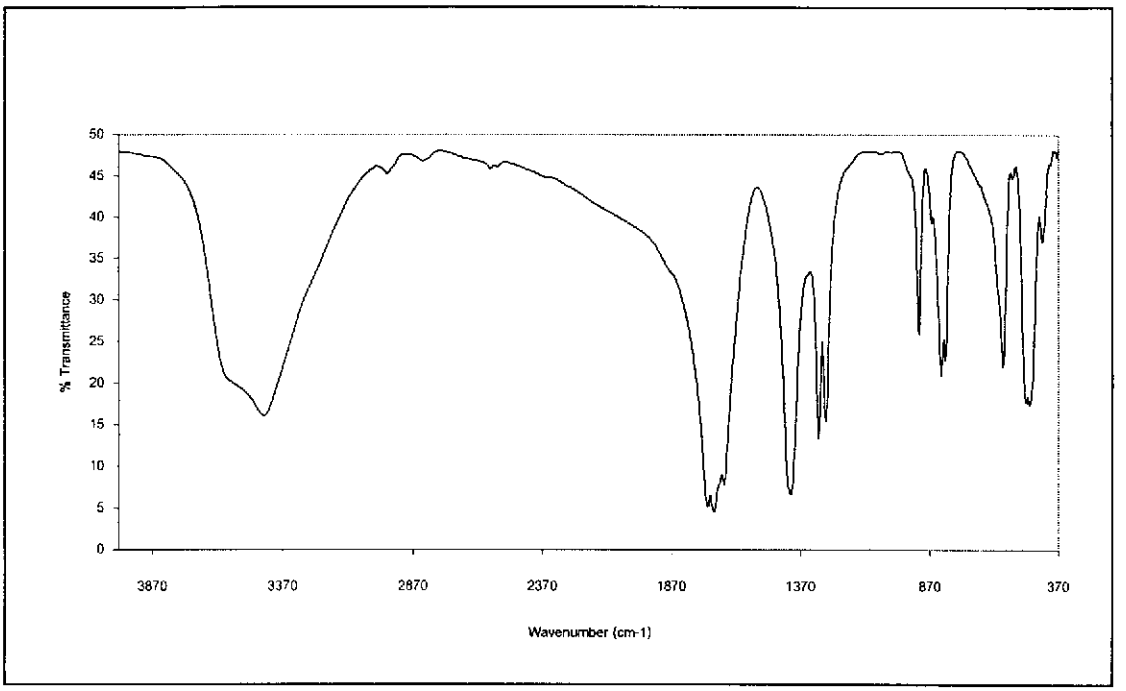

Figure 14 IR spectrum of Blue complex (KBr disc)

Table 10 IR data of $K_3[Cr(C_2O_4)_3] \cdot 3H_2O$, $K_3[Al(C_2O_4)_3] \cdot 3H_2O$, RedCubic, RedRhombo, and Blue complexes.

Vibrational modes	Frequencies (cm^{-1})					
	$K_3[Cr(C_2O_4)_3] \cdot 3H_2O$	$K_3[Al(C_2O_4)_3] \cdot 3H_2O$	RedCubic	RedRhombo	Blue	ν
νa(C=O)	1712	1723	1723	1722	1723	ν_7
νa(C=O)	1682, 1641	1703, 1660	1712, 1694	1690, 1675	1703, 1660	ν_1
νs(CO) + ν(CC)	1392	1405	1408	1402	1404	ν_2
νs(CO) + δ(O-C=O)	1259	1297, 1271	1291, 1274	1303, 1283	1298, 1271	ν_8
ν(CO) + δ (O-C=O)	898	910	916	909	909	ν_3
δ(O-C=O) + ν(MO)	815, 800	821, 806	815	820, 807	823, 802	ν_9

Vibrational modes	Frequencies (cm^{-1})					
	$K_3[Cr(C_2O_4)_3] \cdot 3H_2O$	$K_3[Al(C_2O_4)_3] \cdot 3H_2O$	RedCubic	RedRhombo	Blue	ν
ν(MO) + ν (CC)	543	583	586	580	583	ν_4
δ(O-C=O) + ring def.	486	429	429	436	429	ν_{10}
ν(MO) + ring def.	417	495	500, 481	490, 473	493, 481	ν_{11}

3.2.6 X-ray Powder Diffraction Patterns

The x-ray powder diffraction method is unique in that it is the only analytical method that is capable of providing qualitative and quantitative information about the compounds present in a solid sample. The identification of a species from its powder diffraction pattern is based upon the position of the lines (in terms of θ or 2θ) and their relative intensities (Skoog and Leary, 1992). The XRD patterns of $K_3[Cr(C_2O_4)_3] \cdot 3H_2O$ and $K_3[Al(C_2O_4)_3] \cdot 3H_2O$ are shown in Figures 15 and 16, respectively. The XRD patterns of both complexes were similar to file 38-1446 of standard reference file with space group $P2_1/c$.

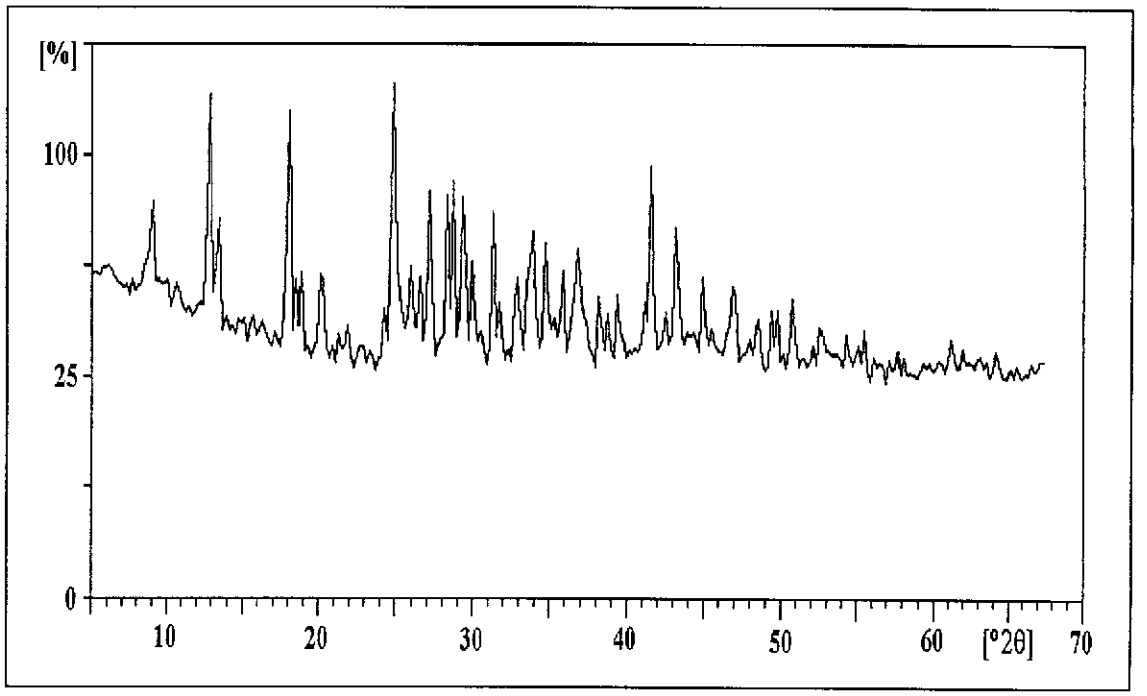

Figure 15 X-ray diffraction pattern of $K_3[Cr(C_2O_4)_3] \cdot 3H_2O$ complex from powder technique

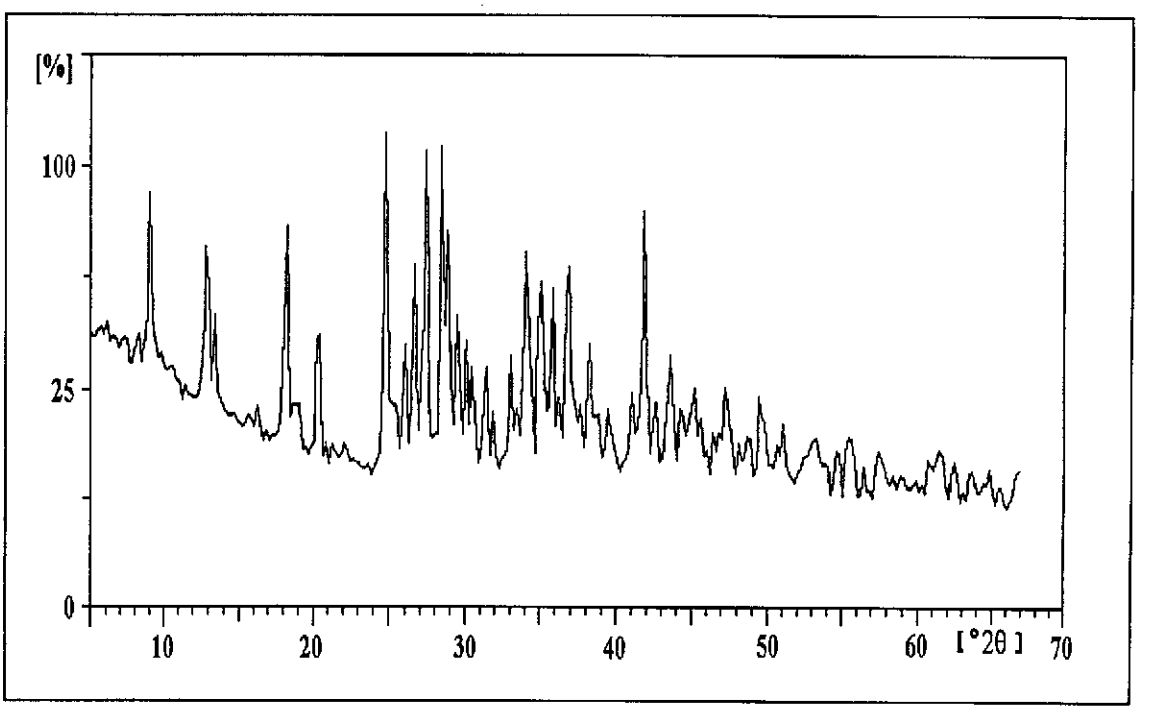

Figure 16 X-ray diffraction pattern of $K_3[Al(C_2O_4)_3] \cdot 3H_2O$ complex from powder technique

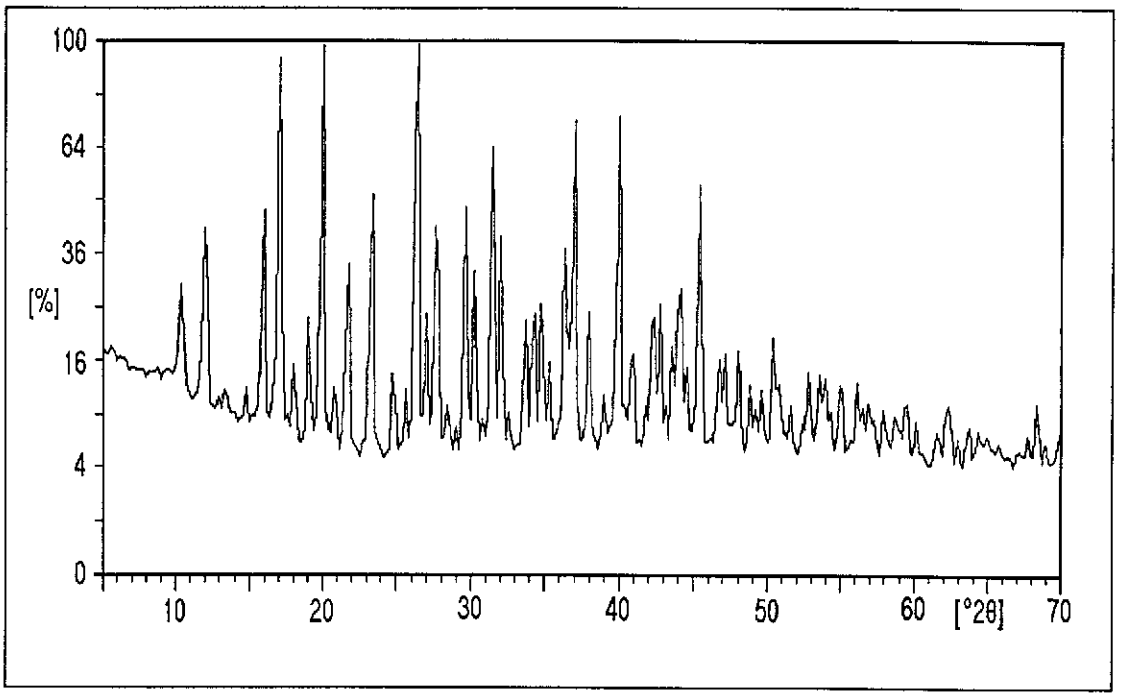

Figure 17 X-ray diffraction pattern of RedCubic complex from powder technique

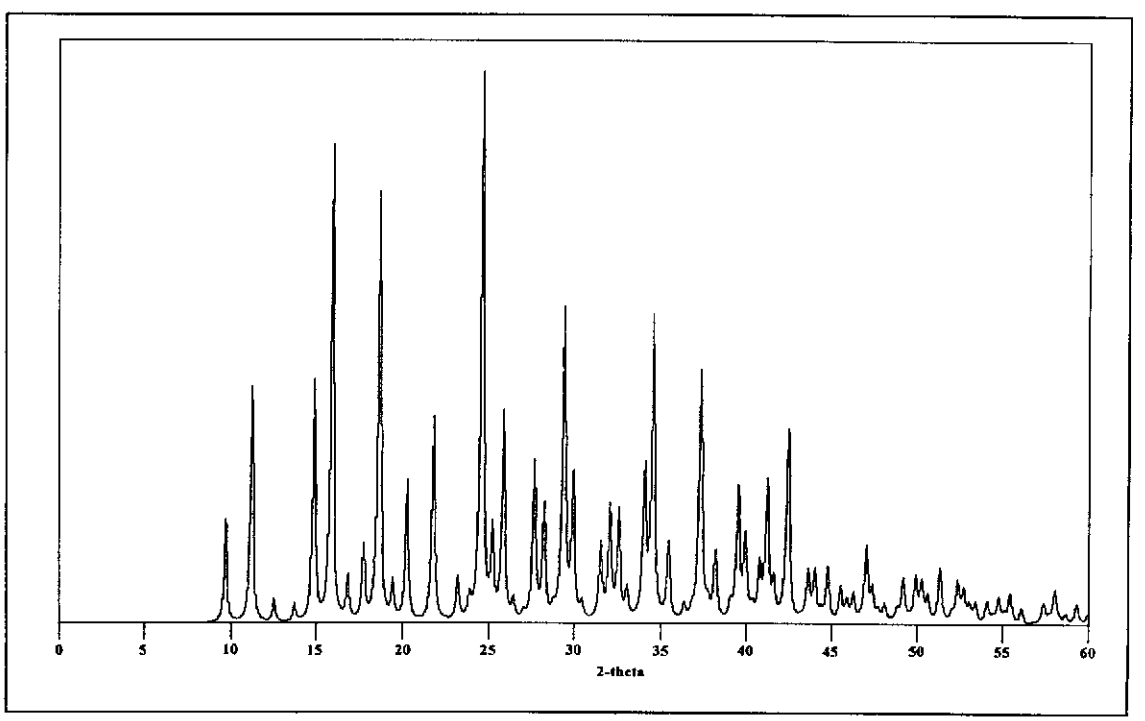

Figure 18 X-ray diffraction pattern of RedCubic complex from single crystal technique

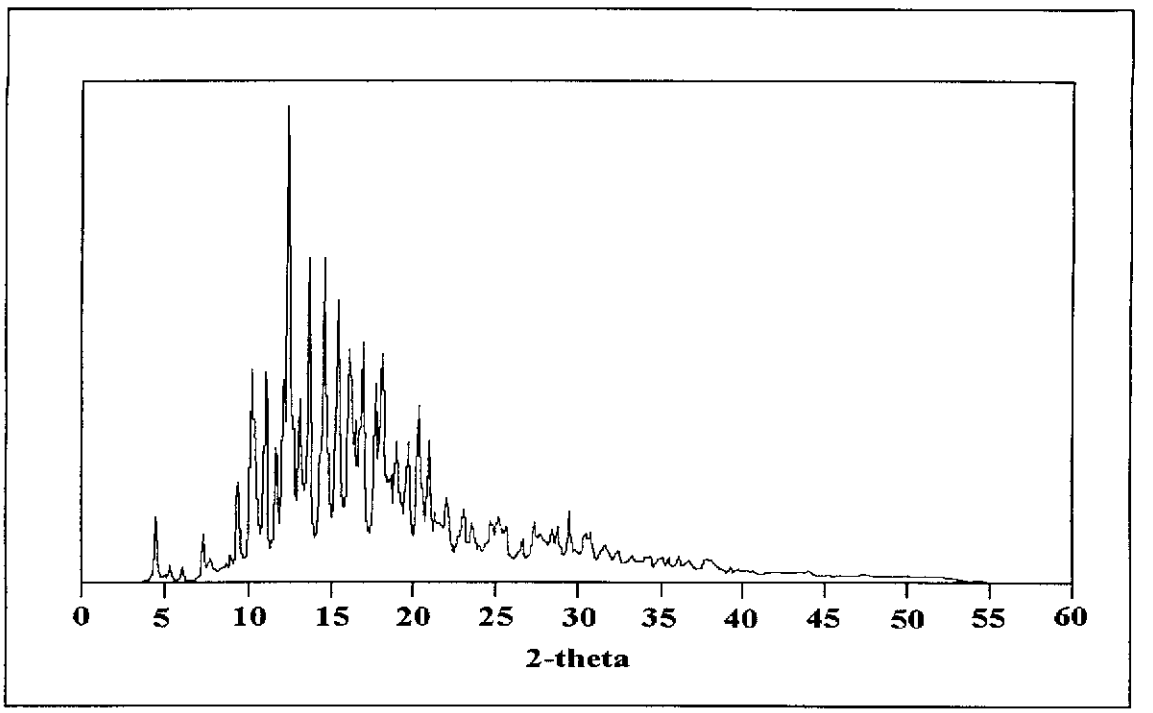

Figure 19 X-ray diffraction pattern of RedRhombo complex from single crystal technique

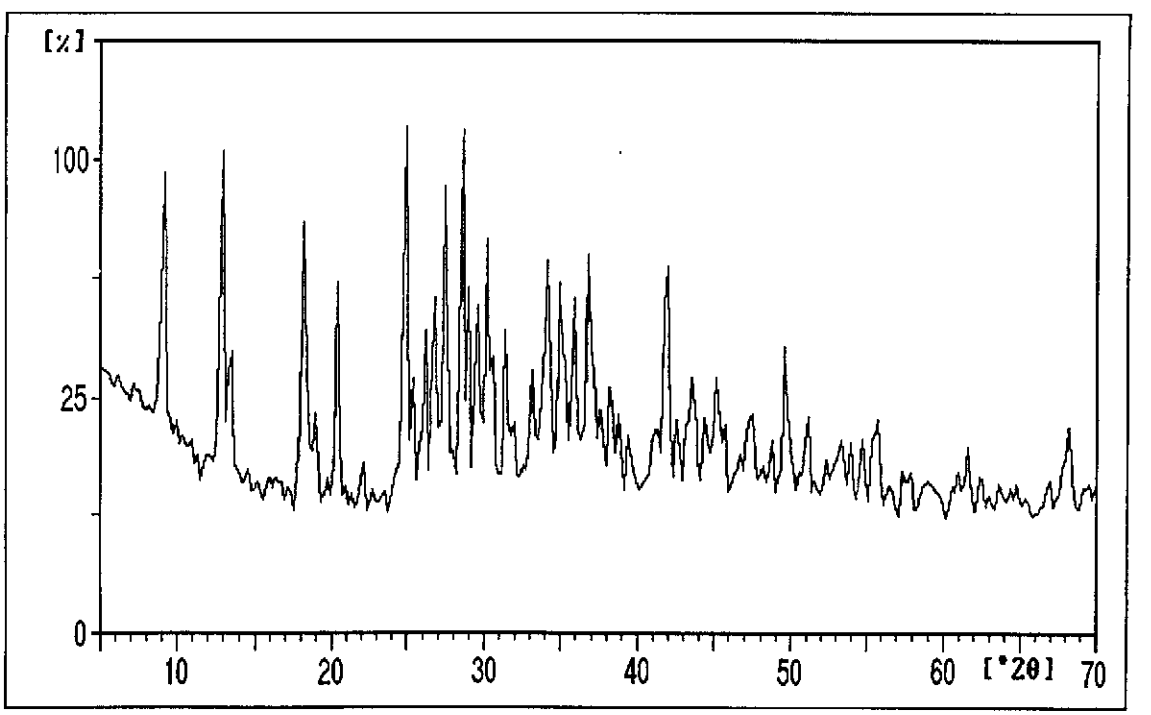

Figure 20 X-ray diffraction pattern of Blue complex from powder technique

3.2.7 Scanning Electron Microscope with Energy dispersive x-ray spectrometer

The SEM/EDX spectrum was acquired through the Scientific Equipment Center, Prince of Songkla University, Hat Yai, Songkla, using a scanning electron microscope, JSM-5800LV, JEOL, Japan, with energy dispersive x-ray spectrometer, ISIS300, Oxford Instruments, UK. In Figures 21-23 show the SEM/EDX spectrum of RedCubic, RedRhombo, and Blue respectively. The element of oxalato complexes are listed in Table 11.

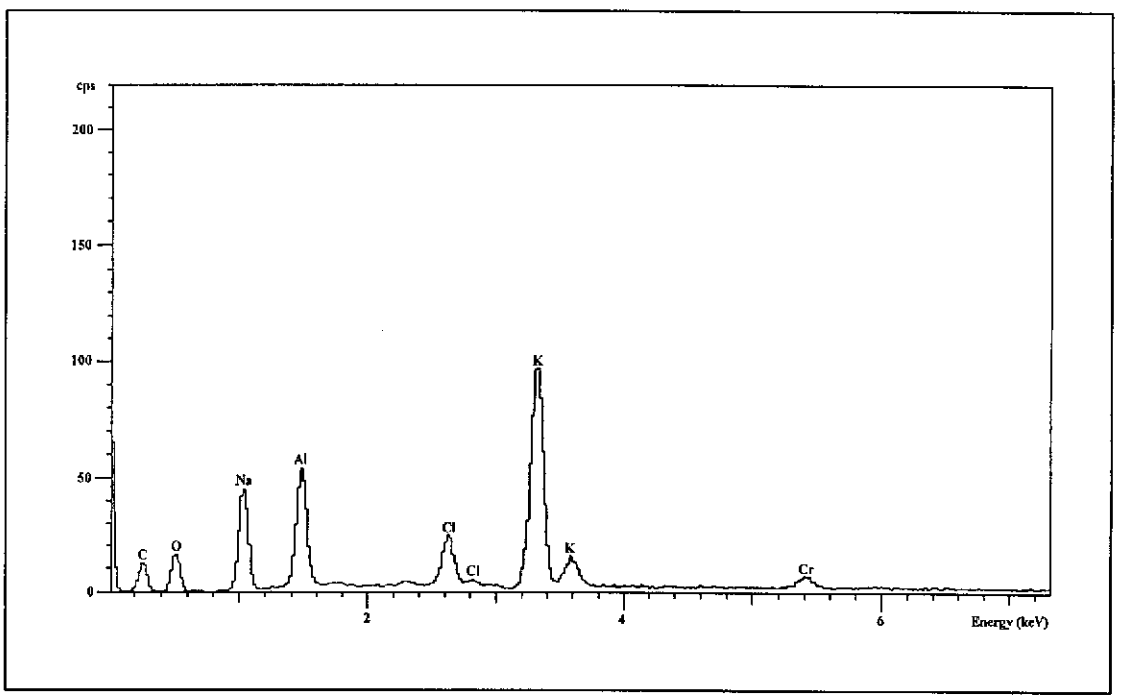

Figure 21 SEM/EDX spectrum of RedCubic complex

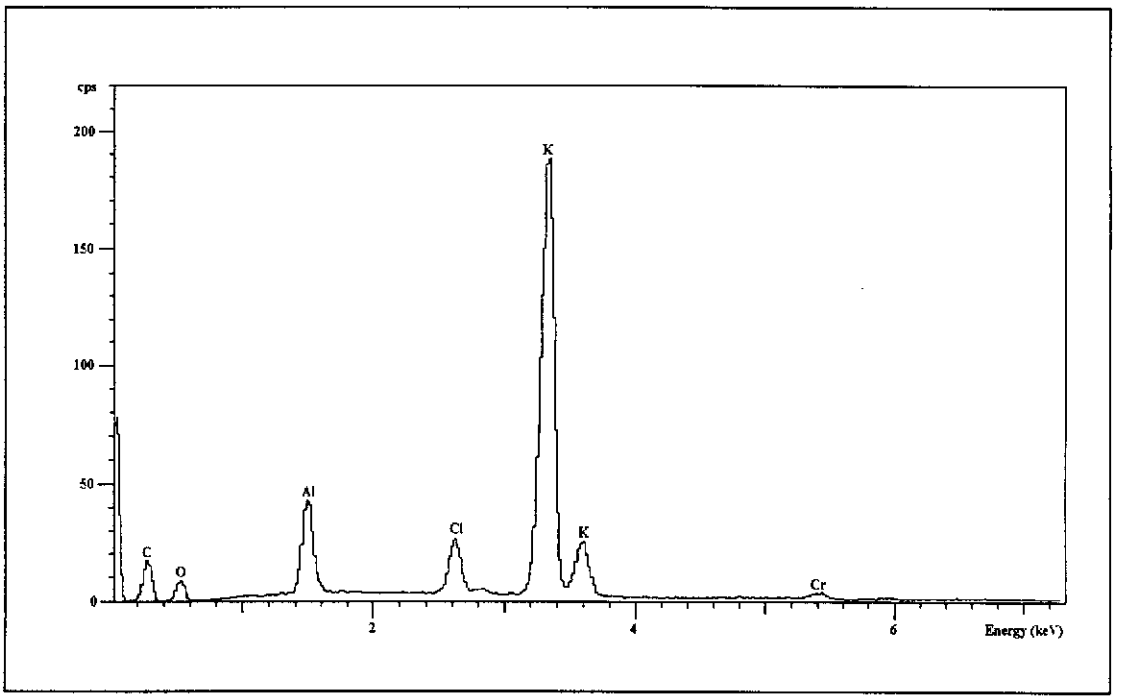

Figure 22 SEM/EDX spectrum of RedRhombo complex

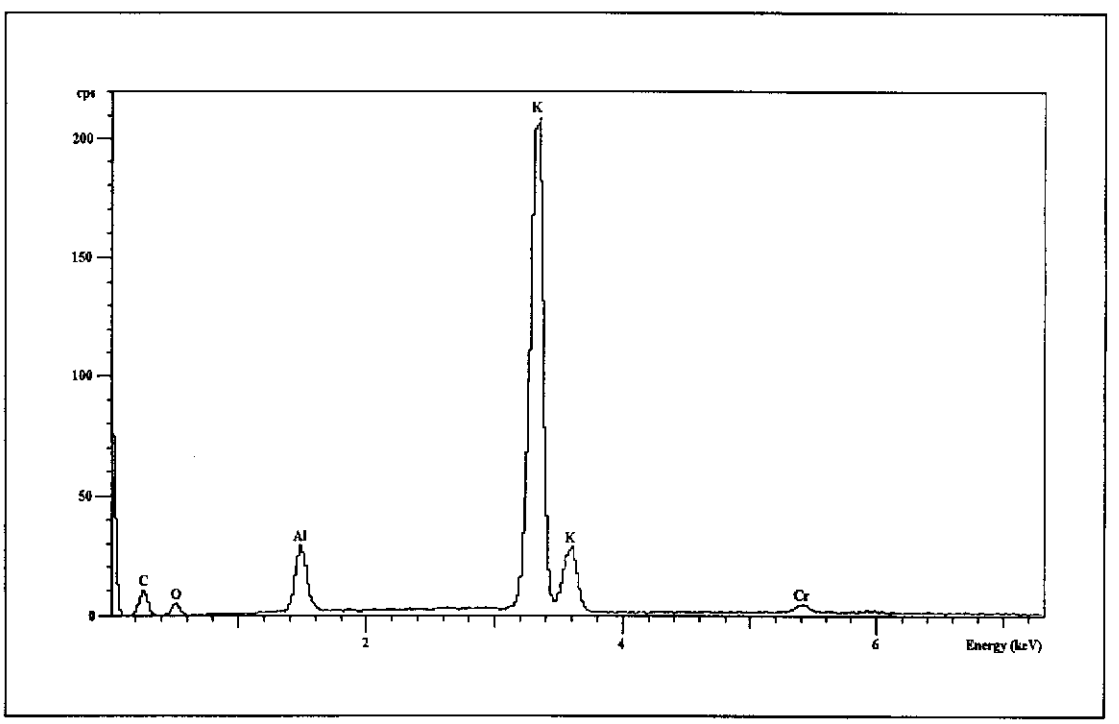

Figure 23 SEM/EDX spectrum of Blue complex

Table 11 The elements in oxalato complexes as found by SEM/EDX

complex	element
$K_3[Al(C_2O_4)_3]\cdot 3H_2O$	C, O, K, Al
$K_3[Cr(C_2O_4)_3]\cdot 3H_2O$	C, O, K, Cr
RedCubic	C, O, K, Al, Cr, Cl, Na
RedRhombo	C, O, K, Al, Cr, Cl
Blue	C, O, K, Al, Cr

3.2.8 Thermogravimetric analysis

Thermogravimetric analysis provides the analyst with a quantitative measurement of any weight change associated with a transition. For example, TGA can directly record the loss in weight with time or temperature due to dehydration or decomposition (Willard, et al., 1974). Figures 24 and 25 display TG curve obtained for $K_3[Al(C_2O_4)_3]\cdot 3H_2O$ and $K_3[Cr(C_2O_4)_3]\cdot 3H_2O$, respectively.

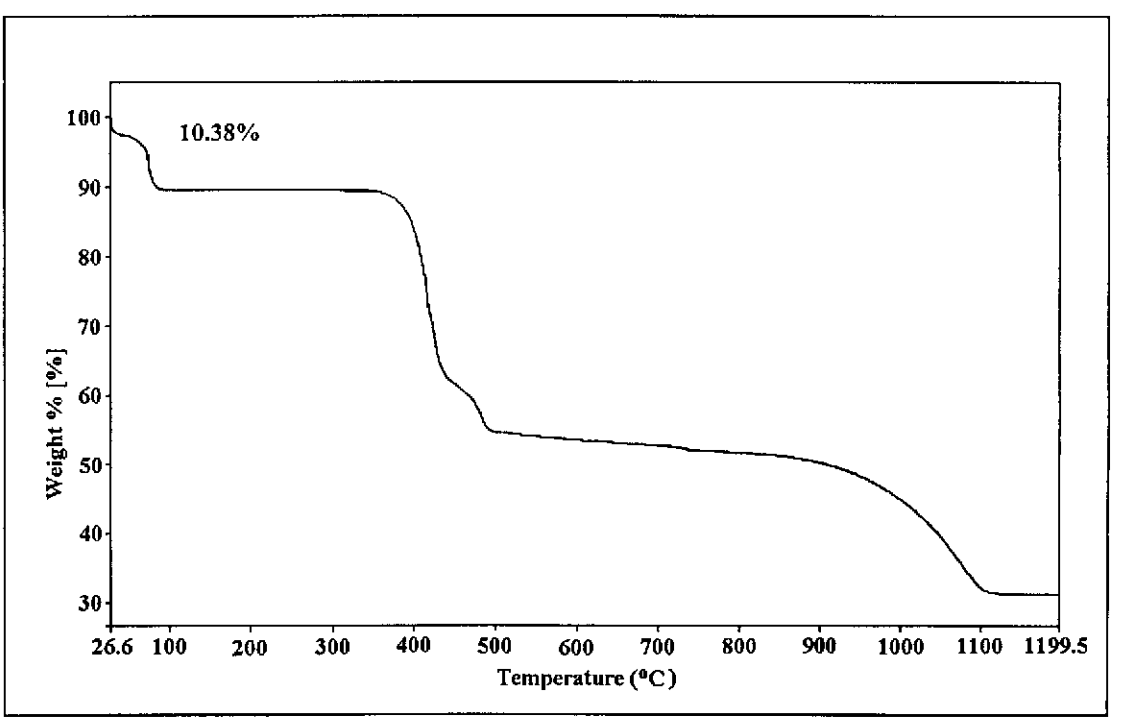

Figure 24 TGA spectrum of $K_3[Al(C_2O_4)_3]\cdot 3H_2O$ complex

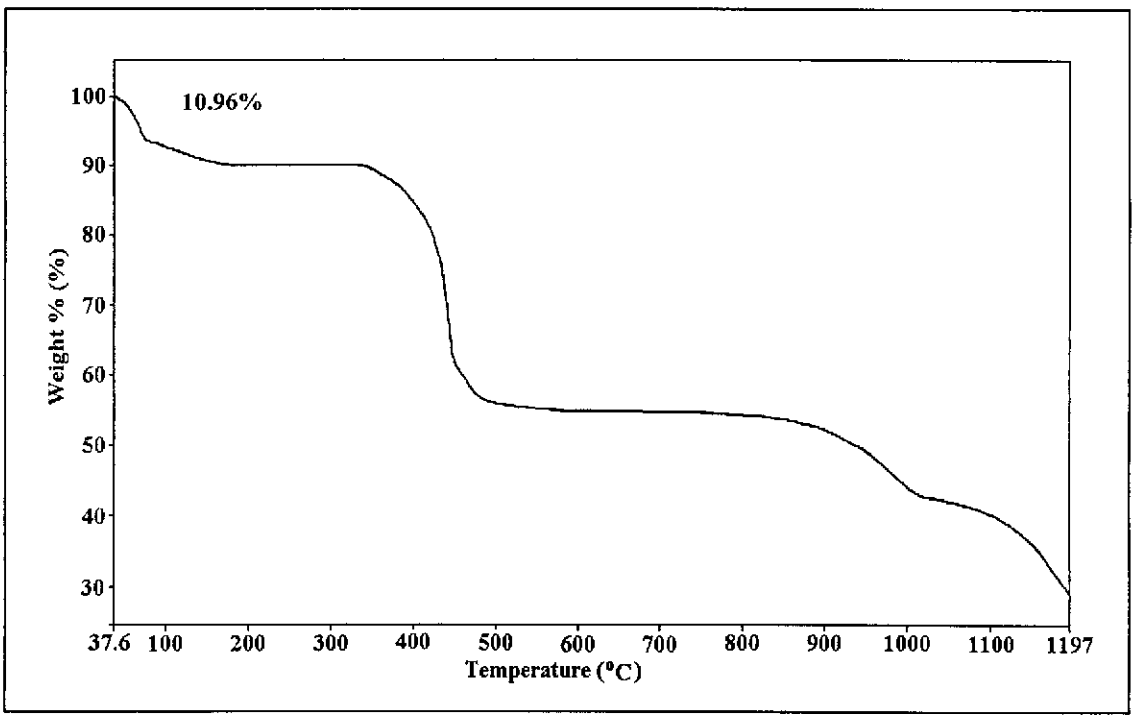

Figure 25 TGA spectrum of $K_3[Cr(C_2O_4)_3]\cdot 3H_2O$ complex

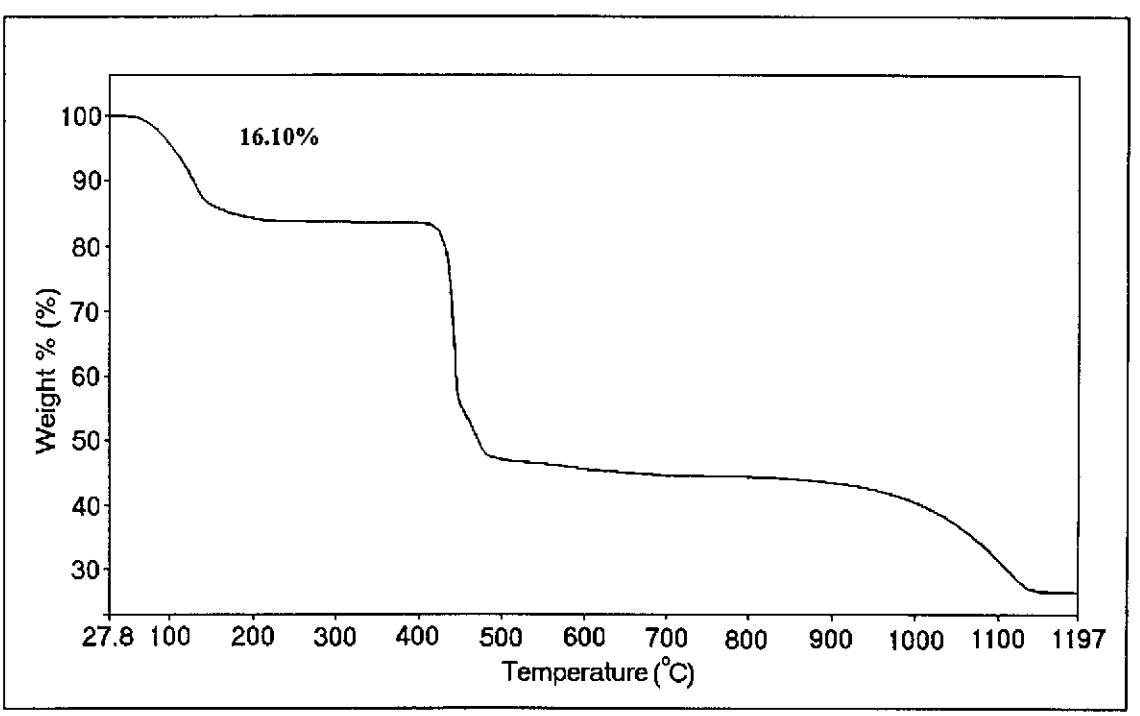

Figure 26 TGA spectrum of RedCubic complex

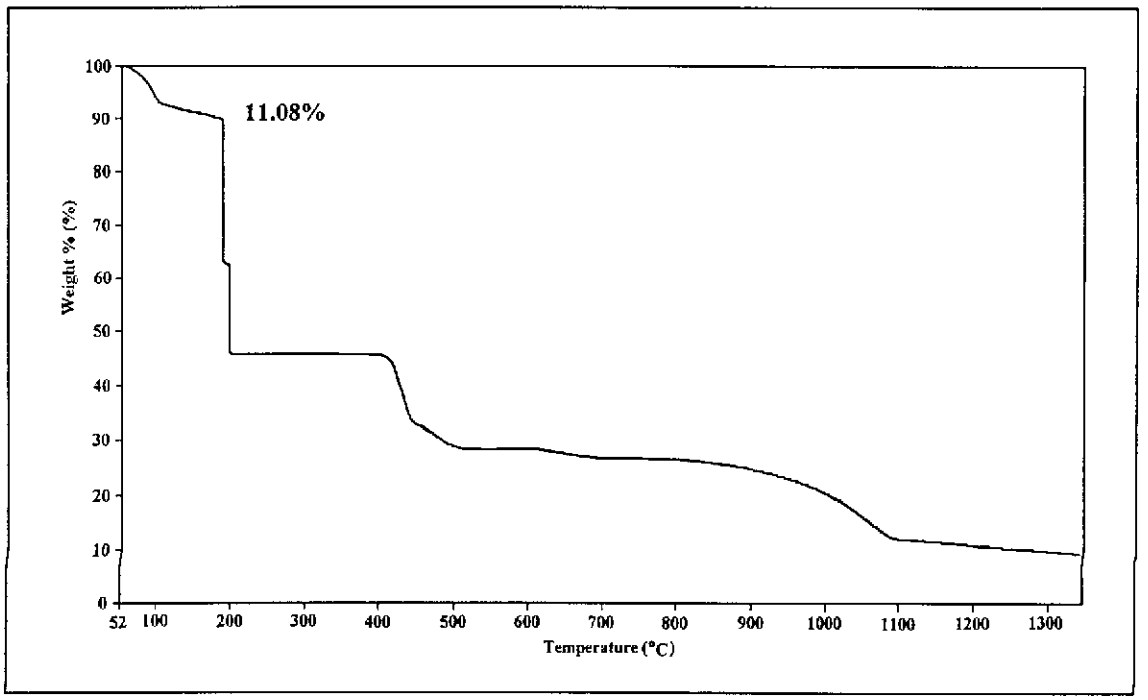

Figure 27 TGA spectrum of RedRhombo complex

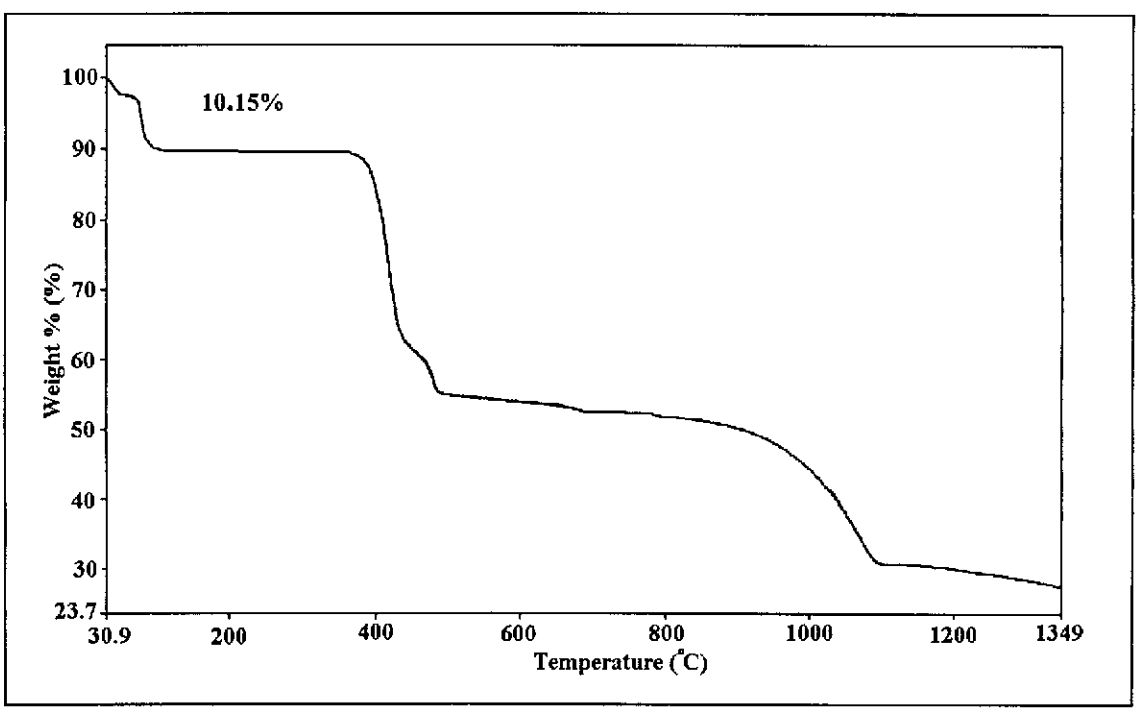

Figure 28 TGA spectrum of Blue complex

Table 12 Summary of the TG results obtained by heating from 30°C to 1200°C at 10° C/min in air.

Complex	First (30-150°C) Mass loss (%)	Second (200-800°C) Mass loss (%)	Third (800-1100°C) Mass loss (%)
$K_3[Al(C_2O_4)_3]3H_2O$	10.38 (11.69)	37.58	20.57
$K_3[Cr(C_2O_4)_3]3H_2O$	10.96 (11.09)	35.26	18.04
RedCubic	16.10	38.79	18.14
RedRhombo	11.08 11.35	64.69	16.11
Blue	10.15	37.34	22.35

3.2.9 Differential scanning calorimeter

DSC is a thermal technique in which differences in heat flow into a substance and a reference are measured as a function of sample temperature while the two are subjected to a controlled temperature program (Skoog and Leary, 1992). The DSC spectra of $K_3[Al(C_2O_4)_3].3H_2O$, $K_3[Cr(C_2O_4)_3].3H_2O$, RedCubic, RedRhombo, and Blue crystals are shown in Figures 29-33, respectively, and summarized in Table 13.

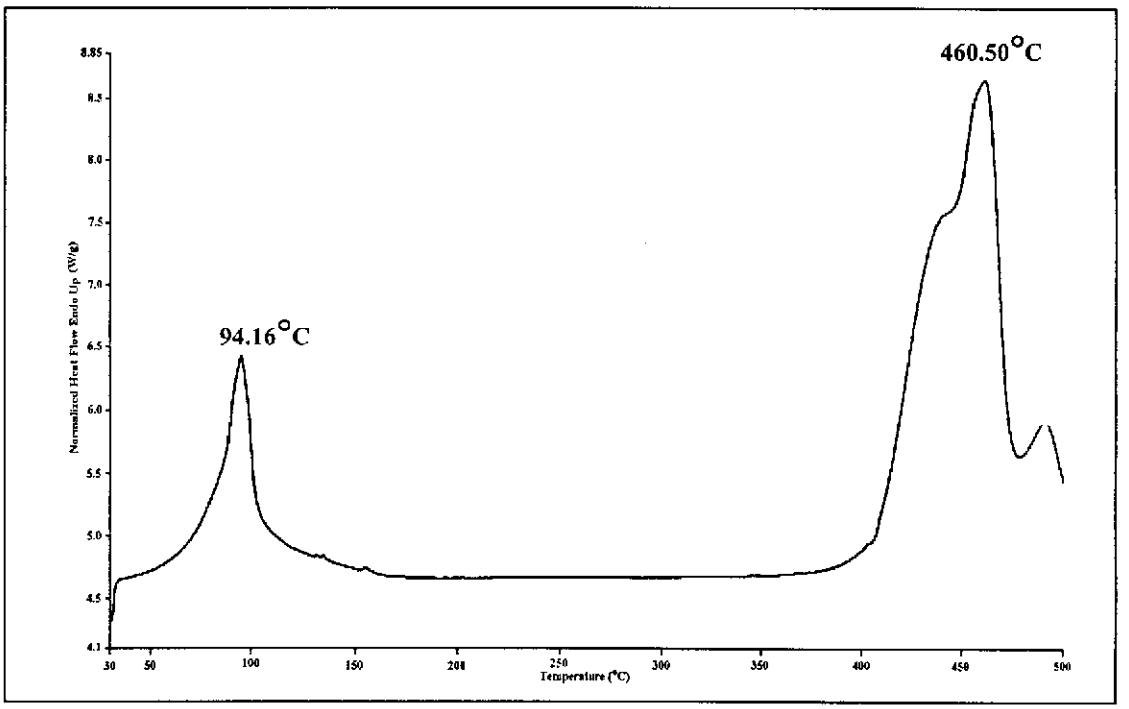

Figure 29 DSC spectra of $K_3[Al(C_2O_4)_3]3H_2O$ complex

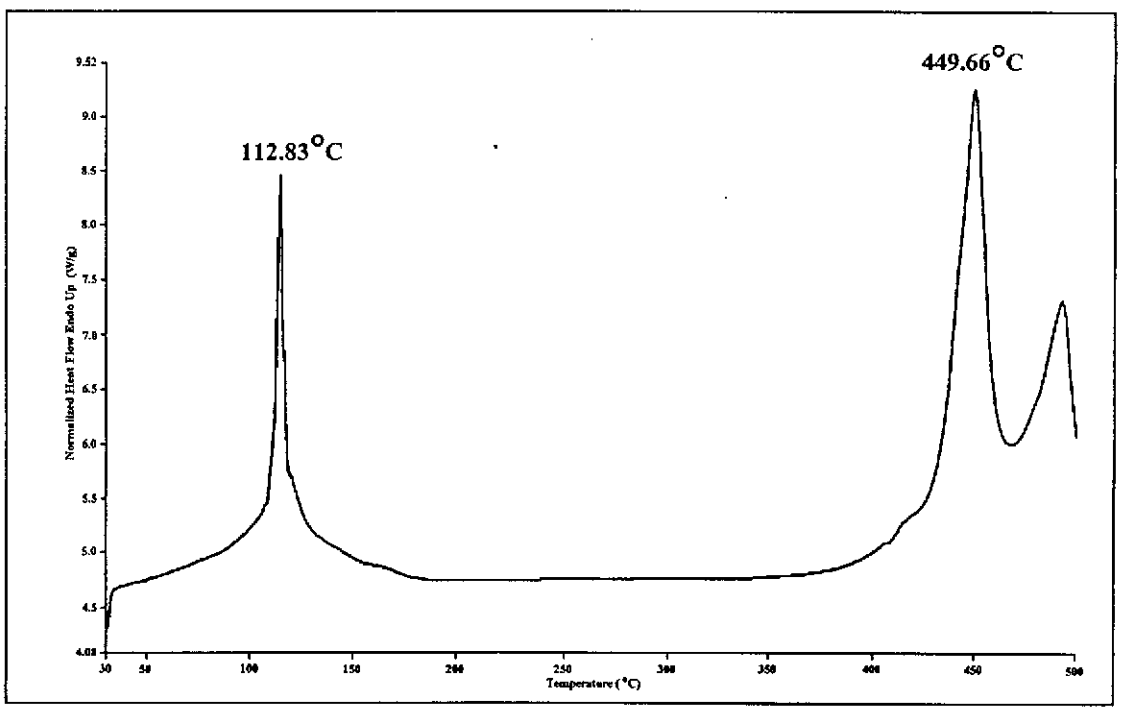

Figure 30 DSC spectrum of $K_3[Cr(C_2O_4)_3]3H_2O$ complex

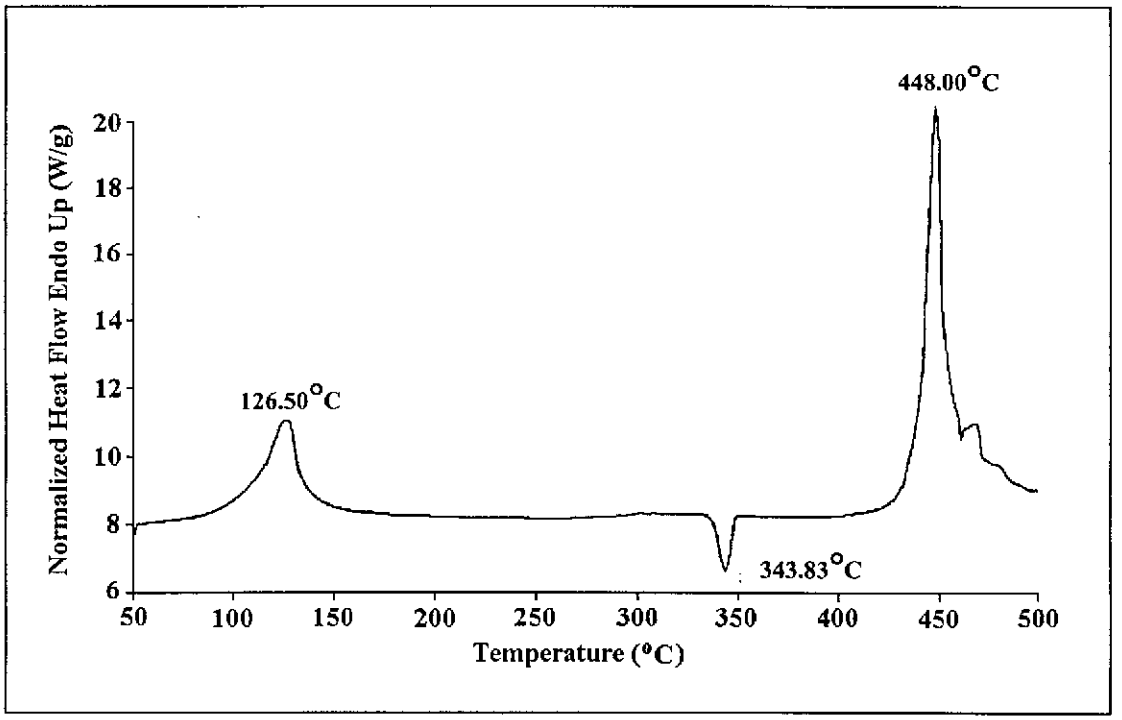

Figure 31 DSC spectra of RedCubic complex

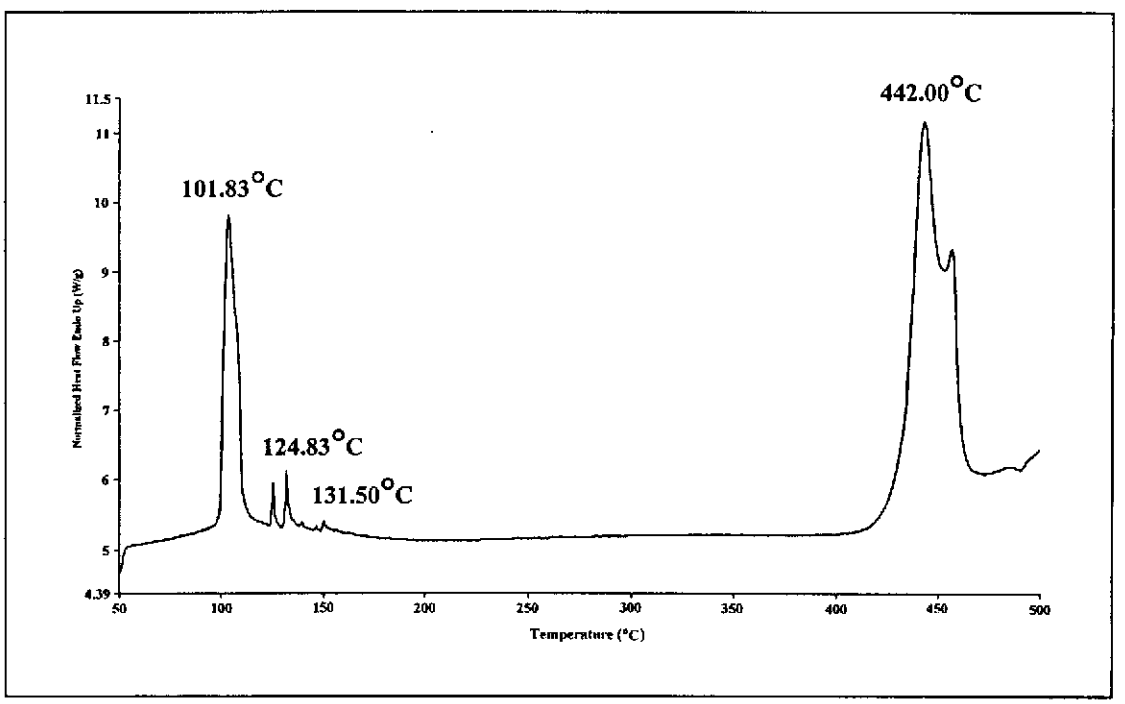

Figure 32 DSC spectra of RedRhombo complex

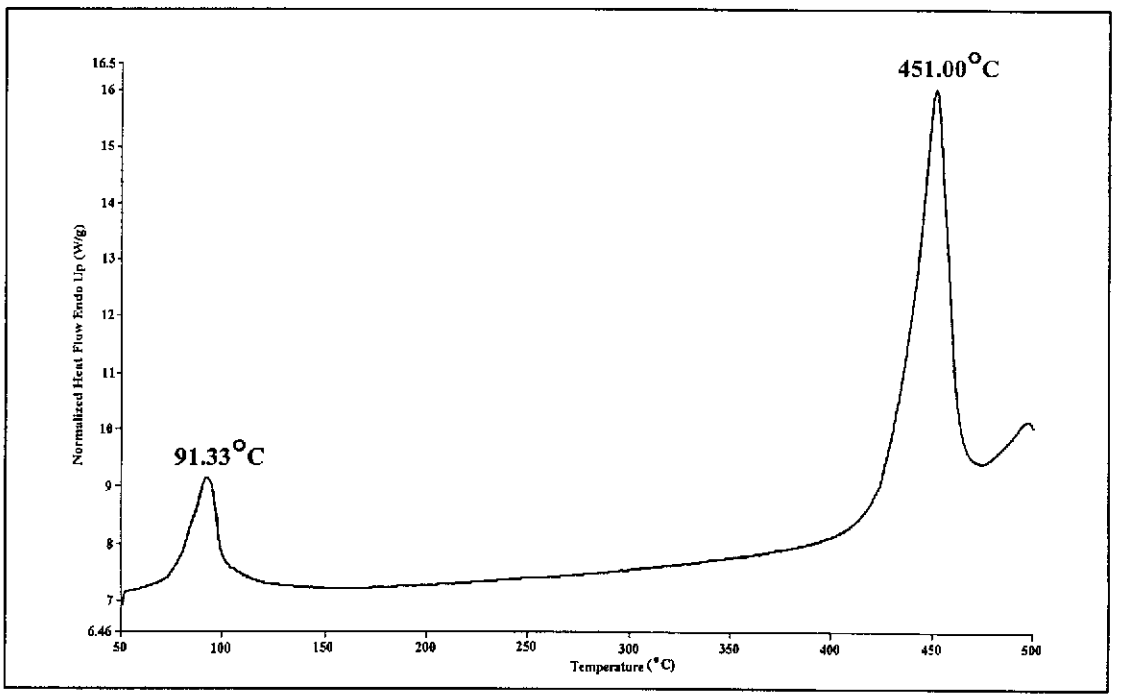

Figure 33 DSC spectra of Blue complex

Table 13 Summary of the DSC results obtained by heating from 30°C to 500°C at 10°C/min in air.

Complex	First		Second	
	area, J/g	Temperature, °C	area, J/g	Temperature, °C
$K_3[Al(C_2O_4)_3]3H_2O$	290.29	94.16	845.02	460.50
$K_3[Cr(C_2O_4)_3]3H_2O$	306.95	112.83	872.47	449.66
RedCubic	417.15	126.50	1039.63	448.00
RedRhombo	201.66	101.83	636.13	442.00
	5.32	124.83		
	8.72	135.50		
Blue	195.42	91.33	839.62	451.00